# Development of an active peptide derived from the Sacsin J domain and identifying new functions of Sacsin in ARSACS models

#### Alexandre Paré

Integrated Program in Neuroscience

Montreal Neurological Institute

Dep of Kinesiology and Physical Education

Dep of Neurology and Neurosurgery

McGill University

Montreal, Quebec, Canada

July 2023

A thesis submitted to McGill University in partial fulfilment of the requirements of the degree of Master of Science

© Alexandre Paré 2023

# Table of Contents

ABSTRACT – ENGLISH	5
RÉSUMÉ – FRANCAIS	6
ACKNOWLEDGMENTS	7
CONTRIBUTION OF AUTHORS	8
LIST OF FIGURES	9
LIST OF ABBREVIATIONS:	12
SECTION 1: INTRODUCTION AND STATEMENT OF PROBLEM	15
SECTION 2: BACKGROUND LITERATURE	16
ARSACS IS A NEUROLOGICAL DISORDER CAUSED BY MUTATIONS IN THE GIANT SACS GENE	16
ARSACS Models	17
OVERVIEW OF SACSIN FUNCTIONS	18
Sacsin Structural Organization and Domain Functions	18
Sacsin Role in Cytoskeletal Dynamics	19
Sacsin's Role in Mitochondria	22
Sacsin Role in Autophagy	23
Sacsin Role in Protein Transport	24
ROLE OF RAB1 IN THE SECRETORY PATHWAY	25
Secretory Pathway General Overview	25
RAB Protein Family and Molecular Mechanism Functions in Secretory Pathway Trafficking	26
PTMs and Regulation of Rab Activity	27
RAB 1 Functions in Secretory Pathway Trafficking	29
Role of RAB1 in Autophagy	30
Involvement of Rab1 in Neurodegenerative Diseases	30

SECTION 3: RATIONALE, HYPOTHESIS, AND SPECIFIC AIMS	31
SECTION 4: METHODS	32
SECTION 5: RESULTS	38
AIM 1: TO CHARACTERIZE THE DOSE-RESPONSE AND TEMPORAL EFFECT OF A TAT-SACSJ PEPTIDE TRE	ATMENT
ON IF NETWORK IN ARSACS CELLULAR MODELS	38
A Cell-Permeant SacsJ Peptide captures the dynamics of Vimentin disassembly in Fibroblasts .	38
SacsJ Disassembles NF in Murine MNs in Culture	40
AIM 2: TO IDENTIFY INTERACTORS OF THE SACSJ DOMAIN AND TO DETERMINE IF THEIR EXPRESSION IS	
DYSREGULATED IN ARSACS MODELS	40
Proteomic Analysis of the SacsJ Interactome Identifies a Role in Membrane Dynamics and Ra	ab1b as a
Most Abundant Binding Partner	40
AIM 3: TO CHARACTERIZE THE ROLE OF RAB1 AND THE EFFECT OF LACK OF SACSIN ON DISTRIBUTION (	OF
SECRETORY PATHWAY ORGANELLES (ER, ERGIC, GOLGI AND AUTOPHAGY) AND IF SACSJ OR OTHER SA	ACSIN
DOMAINS CAN RESTORE RAB1 SUBCELLULAR LOCALIZATION.	41
Absence of Sacsin Upregulates Rab1b and Restricts its Distribution to the Cell Soma	41
Absence of Sacsin Restricts Distribution of Rab-1 related Organelles	42
Rab1b and Organelles Abnormalities are Direct Targets of Sacsin	43
Sacsin Domains Alter Rab1b Subcellular Distribution and Association with ER in SW13- Sacs-	/- Cells44
Conclusion and Contribution to Original Knowledge	44
SECTION 6: DISCUSSION, CONCLUSION AND FUTURE DIRECTIONS	45
Summary of Main Findings	45
SacsJ and Intermediate Filaments	45
Identification of SacsJ Clients	46
Sacsin Regulate Golgi Morphology through Rab1b	17
Daesin Regulate Ovigi vivi phology univagn Raviv	

Role of Sacsin Domains in the Regulation of Rab1b Functions	48
Conclusion	50
Future Directions	50
SECTION 7: FIGURES	51
SECTION 8: REFERENCES	67

#### **Abstract** – **English**

Autosomal Recessive Spastic Ataxia of Charlevoix Saguenay (ARSACS) is caused by loss of function mutations in the SACS gene, which encodes sacsin, a giant 520 kDa protein. Little is known about sacsin function, but a key feature is the formation of abnormal bundles of intermediate filaments (IF) including neurofilaments (NF) in its absence. The J domain (SacsJ) is a cochaperone that interacts with Hsp70 chaperones; its client proteins are unknown therefore we aimed to determine the role of this domain. Mass spectrometry identification of binding partners of the SacsJ domain, which resolve NF bundles in vitro, show Rab1b protein as a strong interactor involved in organelle trafficking. Rab1 is responsible for regulating trafficking activities between the ER, Golgi and ATG9 autophagic vesicles, which morphologies and cellular distributions are affected by the lack of sacsin in motor neurons (MN) in culture and in vivo. Because IF plays a role in the regulation of these organelles' morphologies, Adenocarcinoma SW13<sup>vim-/-</sup> (abbreviated as SW13- for the rest of my thesis) knocked out for sacsin and lacking IF were used to demonstrate the independence of Golgi compaction to IF bundling. In SW13- Sacs-/-, expression of the SacsJ<sup>H33Q</sup> (hsp70 binding incompetent SacsJ mutant), and Ubl domains increase localization of Rab1 to the ER. Our data identifies new interacting partners of the DNAJ domain and show the role of SacsJ and other sacsin domains in ER/Golgi trafficking independently of IF protein.

#### Résumé – Français

L'ataxie spastique récessive autosomique de Charlevoix Saguenay (ARSACS) est causée par des mutations de perte de fonction dans le gène SACS, qui code pour sacsin, une protéine géante de 520 kDa. On sait peu de choses sur la fonction de la sacsin, une caractéristique clé est la formation de faisceaux anormaux de filaments intermédiaires (IF), y compris les neurofilaments (NF) en son absence. Le domaine J (SacsJ) est un cochaperon qui interagit avec les chaperons Hsp70; ses protéines clientes sont inconnues, nous avons donc cherché à déterminer le rôle de ce domaine. L'identification par spectrométrie de masse des partenaires de liaison du domaine SacsJ, qui résolvent l'agglomération pathologique de NF in vitro, montre que la protéine Rab1b est un interacteur abondant impliqué dans le trafic des organelles. Rab1 est responsable de la régulation des activités de trafic entre les vésicules autophagiques ER, Golgi et ATG9, dont les morphologies et les distributions cellulaires sont affectées par le manque de sacsin dans les motoneurones en culture et in vivo. Parce que l'IF joue un rôle dans la régulation des morphologies de ces organelles, la ligné cellulaire adénocarcinomes SW13- knock-out pour la sacsin et dépourvu d'IF a été utilisé pour démontrer l'indépendance du compactage de Golgi par rapport à l'agglomération des IF. Dans SW13- Sacs-/-, l'expression des domaines SacsJ, H33Q (mutant DNAJ incompétent pour la liaison Hsp70) et Ubl augmente la localisation de Rab1 dans le réticulum endoplasmique (RE). Nos données démontrent pour la première fois le partenaire d'interaction du domaine DNAJ et le rôle de SacsJ et d'autres domaines sacsin dans le trafic RE/Golgi indépendamment de la protéine IF.

# Acknowledgments

I am incredibly excited and grateful to have completed my master's degree after submitting this thesis and contributing to the advancement of science. I would first like to thank my mentor and supervisor Dr. Benoit Gentil who took a chance on a curious undergraduate football player. You have provided me with an amazing opportunity and an incredible purpose. Your continuous support throughout my research and other endeavors has been life changing; your guidance, enthusiasm, and friendship have not only shaped my development as a researcher but allowed me to blossom as human being as well.

I would like to thank all members of the Durham and Gentil Lab: Nancy Larochelle, Sandra Minotti, Heather Durham, Zacharie Cheng-Boivin, and Mario Fernandez. Your support and ideas have been crucial in the completion of my thesis. A special thank you to Sandra Minotti, you are the cornerstone of our lab. I cannot express enough how much I appreciate everything you do to support us in our experiments. The preciseness and attention to detail that define your work greatly influence the way I operate. Special mention to Nancy for your help with Western Blots, bubbles begone.

I want to thank the members of my advisory committee: Heather Durham, Gary Armstrong, and Alanna Watt. Your insights and encouragements have pushed me to think deeper and motivate me to undertake new challenges. Heather, I cherish our individual meetings and want to thank you for your patience and help in the writing of this thesis. Benoit and you have rebuilt the way I think and write, and for that, I am incredibly grateful.

# **Contribution of Authors**

AP: Alexandre Paré, BG: Benoit Gentil, HD: Heather Durham, AD: Afrooz Dabbaghizadeh

# **Section 1: Introduction and Statement of Problem**

AP wrote this section in collaboration with BG.

Contains excerpts from a published manuscript (Dabbaghizadeh, A., Paré, A., Cheng-Boivin, Z., Dagher, R., Minotti, S., Dicaire, M. J., ... & Gentil, B. J. (2022). The J domain of sacsin disrupts intermediate filament assembly. *International Journal of Molecular Sciences*, 23(24), 15742.)

BG, HD, AD, and AP contributed to the publication.

# **Section 2: Background Literature Review**

AP wrote this section in collaboration with BG.

Contains excerpts from a published manuscript (Gentil, B. J., Lai, G. T., Menade, M., Larivière, R., Minotti, S., Gehring, K., ... & Durham, H. D. (2019). Sacsin, mutated in the ataxia ARSACS, regulates intermediate filament assembly and dynamics. *The FASEB Journal*, *33*(2), 2982-2994.)

# Section 3: Rationale, Hypothesis, and Specific Aims

AP wrote this section in collaboration with BG and HD.

#### **Section 4: Methods**

AP wrote this section in collaboration with BG and HD.

Contains excerpts and methods from published manuscripts (Gentil, B. J., Lai, G. T., Menade, M., Larivière, R., Minotti, S., Gehring, K., ... & Durham, H. D. (2019). Sacsin, mutated in the ataxia ARSACS, regulates intermediate filament assembly and dynamics. *The FASEB Journal*, *33*(2), 2982-2994.)

(Dabbaghizadeh, A., Paré, A., Cheng-Boivin, Z., Dagher, R., Minotti, S., Dicaire, M. J., ... & Gentil, B. J. (2022). The J domain of sacsin disrupts intermediate filament assembly. *International Journal of Molecular Sciences*, 23(24), 15742.)

#### **Section 5: Results**

AP designed and performed experiments, collected, and analyzed data, and wrote the first draft.

AP wrote this section in collaboration with BG and HD.

Contains excerpts from published manuscript (Dabbaghizadeh, A., Paré, A., Cheng-Boivin, Z., Dagher, R.,

Minotti, S., Dicaire, M. J., ... & Gentil, B. J. (2022). The J domain of sacsin disrupts intermediate filament assembly. *International Journal of Molecular Sciences*, 23(24), 15742.)

AP designed experiments and collected data. BG wrote the manuscript.

#### **Section 6: Discussion, Conclusion and Future Directions**

AP wrote this section in collaboration with BG and HD.

# **List of Figures**

**Figure 1A**: Confocal images of MCH74 fibroblasts treated with SacsJ-myc-TAT in a concentration-dependent manner

**Figure 1B**: Bar graph representing the quantitation of the percentage of MCH74 fibroblasts with IF phenotype following peptide treatment

**Figure 2A:** Confocal images of MCH74 fibroblasts in No Treatment, Control, and Treatment conditions

**Figure 2B:** Confocal images of IF perinuclear phenotype

**Figure 2C**: Confocal images of IF dismantled phenotype

**Figure 2D**: Confocal images of IF diffuse phenotype

**Figure 2E**: Confocal images of IF juxtanuclear phenotype

**Figure 2F**: Bar graph representing the quantitation of the percentage of MCH74 presenting different IF phenotypes over time following peptide treatment

**Figure 3A:** Confocal images of NF network in *Sacs+/+* motor neurons following peptide treatment

- **Figure 3B:** Bar graph representing the quantitation of the percentage of *Sacs*+/+ motor neurons with NF phenotype following peptide treatment
- **Figure 4A:** Confocal images of NF network in *Sacs-/-* motor neurons following peptide treatment
- **Figure 4B:** Bar graph representing the quantitation of the percentage of *Sacs-/-* motor neurons with NF phenotype following peptide treatment
- **Figure 5A:** Picture of red ponceau staining following pulldown for spinal cord lysate, GST, and SacsJ
- **Figure 5B:** Venn Diagram representing distribution into specific binding proteins and common partners of GST and DNAJ
- **Figure 5C:** Volcano plot comparing enrichment of different proteins for GST and DNAJ with highlighted Rab1b
- Figure 5D: List of enriched proteins from most (top) to least (bottom) showing Rab1b
- Figure 5E: Interaction map of SacsJ-specific partners using STRING software
- **Figure 5F:** Donut-pie chart indicating major biological functions carried by SacsJ-interacting proteins as defined by GO-terms
- **Figure 6A:** Western blot analysis of Rab1b levels in *Sacs+/+* and *Sacs-/-* mice
- **Figure 6B:** Confocal images showing NF bundles and Rab1b distribution in 6-month-old Sacs+/+ and Sacs-/- mouse MNs
- Figure 7A: Schematic representation of Rab1b role in secretory pathway and autophagy
- **Figure 7B:** Confocal images showing Rab1b distribution in 6-week-old spinal cord *Sacs+/+* and *Sacs-/-* MNs in culture and bar graph representing quantitation of Rab1b distribution phenotype

- **Figure 7C:** Confocal images of ER distribution in *Sacs+/+* and *Sacs-/-* MNs and bar graph representing quantitation of ER distribution phenotype
- **Figure 7D:** Confocal images of ERGIC distribution in *Sacs+/+* and *Sacs-/-* MNs and bar graph representing quantitation of ERGIC distribution phenotype
- **Figure 7E:** Confocal images of Golgi apparatus distribution in *Sacs+/+* and *Sacs-/-* MNs and bar graph representing quantitation of Golgi apparatus distribution phenotype
- **Figure 7F:** Confocal images of ATG9 distribution in *Sacs+/+* and *Sacs-/-* MNs, and bar graph representing quantitation of ATG9 distribution phenotype
- **Figure 7G:** Confocal images of ATG9 and NFL colocalization in *Sacs+/+* and *Sacs-/-* MNs
- **Figure 8A:** Confocal images of Golgi apparatus following Rab1b, Rab1bN121I, BFA treatment in *Sacs+/+* and *Sacs-/-* MNs, bar graph representing quantitation of number of Golgi fragments
- **Figure 9A:** Confocal images of Golgi apparatus distribution in *Sacs+/+* and *Sacs-/-* MNs and NF bundle coursing through Golgi apparatus in *Sacs-/-* MN
- **Figure 9B:** Electron microscopy image of Golgi apparatus in *Sacs+/+* and *Sacs-/-* and NF bundle in proximity to eccentric Golgi in *Sacs-/-*
- **Figure 10A:** Western blot analysis of *Sacs+/+* and *Sacs-/-* SW13- cells show Rab1b levels,
- **Figure 10B:** Confocal images of Golgi apparatus in SW13- Sacs+/+ and Sacs-/- cells with bar graphs representing quantitation of Golgi apparatus phenotype
- **Figure 11A:** Confocal images of colocalization between Rab1b and Golgi apparatus in Sacs+/+ and Sacs-/- SW13- cells
- **Figure 11B:** Confocal images of colocalization between Rab1b and Golgi apparatus in Sacs+/+ and Sacs-/- SW13- cells following Dnaj transfection

**Figure 11C:** Bar graphs representing quantitation of colocalization between Rab1b and Golgi after transfection of specific sacsin domains

**Figure 12A:** Confocal images of colocalization between Rab1b and ER in Sacs+/+ and Sacs-/-SW13- cells

**Figure 12B:** Confocal images of colocalization between Rab1b and ER in Sacs+/+ and Sacs-/- SW13- cells following Dnaj, H33q, Ubl transfection

**Figure 12C:** Bar graphs representing quantitation of colocalization between Rab1b and Golgi after transfection of specific sacsin domains

# **List of Abbreviations:**

α-syn Alpha-SynucleinALS Amyotrophic Lateral Sclerosis

**ARL3** ADP-Ribosylation Factor Like GTPase 3

ARF1 ADP-Ribosylation Factor 1ARF5 ADP-Ribosylation Factor 5

**ARSACS** Autosomal Recessive Spastic Ataxia of Charlevoix Saguenay

**ATX2L** Ataxin-2-like

**ATG9A** Autophagy-Related Protein 9A

**BFA** Brefeldin A

COPI Coat Protein Complex 1
COPII Coat Protein Complex 2

**CYFP1** Cytoplasmic FMR1 interacting protein

DCN Deep Cerebellar NucleiDRG Dorsal Root GangliaDrp1 Dynamin-Related Protein 1

EB1 End-Binding Protein 1
EB3 End-Binding Protein 3

**ECL** Enhanced Chemiluminescence

**ER** Endoplasmic Reticulum

**ERAD** Endoplasmic Reticulum Associated Degradation

**ERES** Endoplasmic Reticulum Exit Sites

**ERGIC** Endoplasmic Reticulum Golgi Intermediate Compartment

**FBS** Fetal Bovine Serum

**FTD** Frontotemporal Dementia

**GAP** GTPase-Activating Protein

GBF1 Golgi-Specific Brefeldin A-Resistance Guanine Nucleotide Exchange

Factor 1

GDI GDP Dissociation Inhibitor
GDF GDI Displacement Factor

**GEF** Guanine Nucleotide Exchange Factors

GGT Geranylgeranyl Transferase
GM130 130-kDa Golgi Matrix Protein
GOLDU3

**GOLPH3** Golgi Phosphoprotein-3

**H33Q** HSP70 Binding-Incompetent Dominant-Negative Mutant of DNAJ

**HEPN** Higher Eukaryote and Prokaryote Nucleotide-Binding

**HIP1R** Huntingtin Interacting Protein 1 Related

HRP Horseradish PeroxidaseHSP Heat Shock Protein

**IPTG** isopropyl-1-thio-β-D galactopyranoside

ITGA1 Integrin Subunit Alpha 1
IF Intermediate filament

KO Knockout

**LAMP2** lysosome-associated membrane protein 2

LC3 Microtubule-Associated Protein 1A/1B-light chain 3

LCV Legionella Containing Vacuole LRRK2 Leucine-rich repeat kinase 2

MN Motor Neuron

MRI Magnetic Resonance Imaging

MT Microtubule NF Neurofilament

P115 General Vesicular Transport Factor p115

P62 Ubiquitin-Binding Protein p62PCC Pearson Correlation Coefficient

PD Parkinson Disease PT Physical Therapy

PTM Post-translational Modification
OCT Optical Coherence Tomography
Rab1O67L GTP-Restricted Rab1b Mutant

**Rab1bN121I** Dominant-Negative Rab1b with Impaired Guanine Nucleotide Binding

**REP** Rab Escort Protein

**RILP** Rab Interaction Lysosomal Protein

ROS Reactive Oxygen Species
SacsJ J Domain of Sacsin

SH3GL2 EndophilinA1

SIRPT Sacsin Internal Repeat Region

**SNARE** Soluble N-Ethylmaleimide-Sensitive Factor Attachment Protein Receptors

**STMN1** Stathmin **SQSTM1** Sequestome 1

**TAK1** Transforming growth factor-β (TGF-β)-activated kinase 1

**TBS** Tris-Buffered Saline

**TMRM** Tetramethylrhodamine Methyl Ester

TGN Trans Golgi Network
UBL Ubiquitin-Like Domain

**ULK** Unc-51-like Autophagy Activating Kinase

VTC Vesicular Tubular Cluster

# **Section 1: Introduction and Statement of Problem**

The autosomal recessive spastic ataxia of Charlevoix-Saguenay (ARSACS), caused by mutations in the SACS gene, has a high prevalence in northeastern Quebec, more specifically the Charlevoix-Saguenay region, and is now described worldwide [1]. Because ARSACS is an autosomal recessive disorder, it is caused by loss-of-function mutations of the SACS gene reflected by the absence or reduced expression of the giant 520kDa protein sacsin. ARSACS is characterized by a triad of main symptoms which are progressive early onset cerebellar ataxia, spasticity, and peripheral neuropathy [2,3]. Currently, management of ARSACS symptoms is through oral medications and physical therapy, the goal being to delay major functional disabilities [4]. There are currently no effective treatments for ARSACS that address the cause of the disease and knowledge of sacsin function is still emerging. Our lab previously demonstrated that one of the sacsin domains carrying Hsp40 co-chaperone homology, called SacsJ, was particularly efficient in resorbing cytoskeletal intermediate filament abnormalities, a key molecular biomarker of ARSACS caused by the lack of sacsin. This project explored the interactome of SacsJ in order to understand its function in intermediate filament regulation. We identified a novel interaction between SacsJ and Rab1b. The functional characterisation of this interaction shed light onto a new role of sacsin in membrane trafficking, which we explored with respect to the regulation of ER-Golgi trafficking.

# **Section 2: Background Literature**

# ARSACS is a Neurological Disorder Caused by Mutations in the Giant SACS Gene

ARSACS was first described by Bouchard et al. in 1978 from a cohort of approximately 325 French-Canadian individuals in 200 families native to the Saguenay Lac St-Jean area of Quebec. Although most cases are in the Quebec region, ARSACS has been genetically confirmed worldwide and is now considered the second most common recessive ataxia after Friedrich's ataxia with a birth incidence of 1:1,932 [1,3,5,6,7]. ARSACS is inherited in an autosomal recessive manner; children have a 25% chance of inheriting the disease if both parents are heterozygous for a SACS pathogenic variant and genetic testing serves to confirm the disease. In ARSACS patients, the SACS gene carries missense, nonsense, or frameshift mutations leading to impaired coding for sacsin [8,9]. ARSACS is a progressive childhood-onset disease typically diagnosed at six years old and identified by the typical triad of cerebellar ataxia, peripheral neuropathy, and pyramidal tract signs [3,7,10,11,12,13,14]. The first sign of the disease is usually slowly progressive cerebellar ataxia (96% of affected individuals present with the feature) with difficulty walking and gait unsteadiness appearing as early as 12 to 18 months, but sometimes later [5]. Subsequently, spasticity of the lower limbs (75%) and a peripheral neuropathy (97%) characterized by an axonopathy and demyelination, appear in affected individuals. Brain magnetic resonance imaging (MRI) reveals other clinical features, including atrophy of the cerebellar vermis (83% of cases), atrophy of the cerebellar hemispheres, and hypointense bilateral stripes in the paramedian pontine reticular formation (49%), a brain structure involved in the coordination of eye movement which could be related to nystagmus, another symptom of ARSACS. ARSACS patients also present with ophthalmologic features; thickened retinal hypermyelinated fibers (33%) identified as yellow

streaks radiating from the edges of the optic disc, and a thicker-than- average peripapillary retinal nerve fiber layer (100% sensitivity, 99.4% specificity) revealed by ophthalmic examination and optical coherence tomography (OCT), respectively [1,15,16]. Dysarthria (74%), mild intellectual disabilities (29%), hearing loss (13%), and urinary dysfunctions (34%) are also documented. ARSACS patients are typically wheelchair-bound at 40 years old, and the only life span study to date concluded that life expectancy was shortened to an average of 51 years [17]. Currently, the management of ARSACS symptoms is tailored to the individual's needs as no curative treatments are available. Physiotherapy and exergames, a technology-driven form of exercise, help with gait ataxia [18]. Physical therapy (PT), oral medications such as baclofen, botulinum toxin injections, and orthotic devices employed early in the disease course may help prevent and delay tendon shortening and joint contractures, improve balance and motility, as well as postpone major functional disabilities related to spasticity until severe muscle weakness or cerebellar ataxia predominates [19,20,21].

#### **ARSACS Models**

ARSACS patient-derived fibroblasts and mouse models are used to understand ARSACS pathogenesis. Common cellular phenotypes observed in ARSACS patients' fibroblasts are an altered mitochondrial network, displaying fused mitochondria and altered mitochondrial morphology with reduced mitochondrial oxygen consumption, dysregulated autophagic flux, altered protein localization, and vimentin intermediate filament bundling [2,14,22,23]. The *Sacs* knockout mouse model or homozygous *Sacs*<sup>R272C</sup> knock-in recapitulates ARSACS behavior, and presents with cellular abnormalities observed in ARSACS patient-derived fibroblasts: mitochondrial network and morphology alterations, neurofilament bundling, and abnormal Purkinje cell electrophysiological findings [24,25,26,27,28]. These pathological

modifications serve as biomarkers and are key events of the molecular cascade of ARSACS and illustrate sacsin's multiple functions in the cell. My thesis incorporates ARSACS patients' fibroblasts and motor neurons in murine dissociated spinal cord cultures as ARSACS models.

#### **Overview of Sacsin Functions**

The multi-domain organization of sacsin points to roles in protein chaperoning and quality control pathways, including roles in regulation of cytoskeletal and mitochondrial dynamics, autophagy, neuroinflammation, synaptogenesis, and vesicle trafficking [2,22,23,24,25,29]. For my thesis, I investigated sacsin's role in cytoskeletal network organization and dynamics, protein localization and transport, and autophagy in our ARSACS models.

# **Sacsin Structural Organization and Domain Functions**

Sacsin is ubiquitously expressed and enriched in the cytoplasm of neurons and dermal fibroblasts [25,30]. Sacsin contains a ubiquitin-like domain (UBL) in the N-terminus with suggested roles in regulating protein degradation through the proteasome. Indeed, Parfitt et al. have shown that this UBL domain of sacsin binds to the 20S proteasome using immunoprecipitation and may be functional [31]. Three large sacsin internal repeat regions (SIRPT1,2,3), unique to sacsin, contain heat shock protein (HSP) 90-like domains with chaperone activity [32]. A sequence with weak homology to the XPC-binding domain plays a role in DNA damage discrimination and enhancement of cell survival. The sacsin XPCB domain interacts with the ubiquitin ligase Ube3A, which reinforces the role of sacsin in regulating protein synthesis and degradation [33]. Finally, a J domain (SacsJ) and a single higher eukaryote and prokaryote nucleotide-binding domain (HEPN) are located in the C-terminus. SacsJ is homologous to HSP40 and a member of the co-chaperone J-Domain superfamily, which plays a role in regulating the activity of HSP70. In a bacterial assay in which cooperation between HSP40 and HSP70 allows

growth, the sacsin J domain replaced the function of an HSP70-binding incompetent bacterial HSP40, demonstrating that the SacsJ domain can function as a co-chaperone. In addition, the complex of SacsJ with HSP70 resolved aggregates of poly-glutamine-expanded ataxin-1 variants causing spinocerebellar ataxia type 1 in SH-SY5Y cells, pointing to the role in protein homeostasis [31]. The functions of the HEPN domain are unknown; this domain, usually found in bacteria, is involved in resistance to aminoglycosides antibiotics and nucleotide binding [34]. In the context of sacsin protein, the HEPN domain is proposed to provide a favorable environment for protein folding by inhibiting protein aggregation through its nucleotide-binding domain [29,31,32,34].

#### **Sacsin Role in Cytoskeletal Dynamics**

Intermediate filaments are 10 nm filamentous structures of the cytoskeleton. They are cell-specific, composed of polymers made of more than 50 differentially expressed proteins classified into six groups. For this thesis, my focus is on type III and type IV IF, specifically vimentin and neurofilament proteins, respectively. Vimentin is ubiquitously expressed in mesenchymal cells, including fibroblasts, endothelial cells, and astrocytes, while the three NF proteins (NF-Light, NF-Medium, NF-Heavy) are expressed in the nervous system [35,36,37,38]. The IF proteins share a common structural organization; a central alpha-helical rod domain of approximately 310 amino acids flanked by amino- and carboxy-terminal domains. The central rod domain plays a crucial role in filament assembly; two polypeptides wind around each other in a coiled-coil structure to form dimers, which then associate in a staggered antiparallel fashion to form tetramers. These tetramers next associate end-to-end to form protofilaments, and the final IF contains approximately eight protofilaments arranged in a rope-like structure. Because they are assembled from antiparallel tetramers, both ends of IFs are equivalent, generating an apolar structure with identical plus and minus ends [39]. A particularity of type III IFs is their ability to assemble into filaments

with only a single polypeptide (vimentin). In contrast, the three type IV NF proteins assemble to form heteropolymers [40,41].

Inside the cell, IFs form a dense cytoskeletal network from the perinuclear space extending outward to the plasma membrane. IFs form a scaffold for organelles, including mitochondria, the Golgi complex, and other subcellular structures via their anchorage with the nuclear and plasma membrane. They also play a role in mechanoresistance [2]. Despite their structural roles, IFs are highly dynamic units with multiple functions, including roles in autophagy, migration, adhesion, and interactions with other cytoskeletal components [42,43,44]. Post-translational modifications (PTMs), including phosphorylation and acetylation, regulate the assembly, organization, and function of IFs within the cell [45,46,47]. Mutations in IFs or their interacting proteins lead to diseases such as Epidermolysis Bulbosa Simplex, Giant Axonal Neuropathy, and progeria Alexander disease and have detrimental pathological functions in ARSACS [48,49,50].

In ARSACS, one of the hallmarks of sacsin absence is the collapse of the IF network. IF bundles appear around the nucleus and extending across the cells body into dendrites, pointing to an important role of sacsin in IF organization. Following immunofluorescence labeling, IF bundles are highly fluorescent and easily observed by epifluorescence microscopy. Therefore, our team selected IF bundling as a key biomarker due to its striking appearance, measurability, and critical role as a biomarker of progressive degeneration of neurons. In addition, multiple sacsin-deficient cell types have IF bundles, including ARSACS patients' fibroblasts, motor neurons (MN) of sacsin knockout mice, and astrocytes of C6 rat glioma cells and microglia N9 mouse [27,51].

Our laboratory previously investigated the role of sacsin in IF organization by expressing individual sacsin domains UBL, SIRPT, SacsJ, and HEPN in MNs of dissociated spinal cord

cultures derived from *Sacs-/-* mice. Expression of the UBL domain decreased NF bundles and the NF protein levels without affecting the NF network assembly. Expression of the SIRPT domain increased the length of NF filaments by providing a scaffold for assembly. The SacsJ domain expression disassembled the NF network and prevented assembly, while the HEPN domain generated a cage-like structure by relocalizing the filaments to the cell's periphery [2]. Taken together, these results show different effects of sacsin domains on IF networks, which suggest that these domains may act cooperatively on IF dynamics. Yet, expression of the SacsJ domain was sufficient to resorb IF bundles suggesting that this domain alone may be necessary for rescuing the ARSACS phenotype.

Recently, sacsin was shown to interact and regulate microtubules dynamics (MT), another filamentous component of the cytoskeleton [22]. MTs are found in all eukaryotic cells; they form by polymerizing alpha and beta tubulin dimers into complex filamentous polar structures [52]. MTs play a role in cell shape and movement and provide a platform for directed motor-driven intracellular transport, including the movement of secretory vesicles, organelles, and macromolecular assemblies [53,54]. Sacsin binds to MTs and regulates its dynamics in ARSACS patient-derived fibroblasts [22]. More specifically, MT repolymerization fails in sacsin-deficient fibroblasts treated with depolymerization agent nocodazole, and results in the formation of disorganized, clustered, and non-radial MTs compared to the regular network in control fibroblasts. Furthermore, the growth rate of MTs is slower in sacsin knockout fibroblasts compared to control, as assessed by live imaging of GFP-labeled MT end-binding protein (EB3-GFP). Romano et al. confirmed the role of sacsin in MT regulation and dynamics using a multi-omic profiling approach in sacsin-deficient cells; MTs have increased acetylated alpha-tubulin, increased polymerization, and disordered movement assessed by live cell imaging of EB1-GFP.

The mechanism by which sacsin regulates MTs is still unknown. However, in sacsin knockout cells, lysosomes were peripherally distributed with little juxtanuclear accumulation, suggesting that disruptions in MT dynamics cause the altered intracellular transport of organelles [22]. MTs are also essential for mitochondrial and vimentin distribution, both affected by the lack of sacsin in different cellular ARSACS models. Indeed, lack of sacsin causes mitochondria to accumulate in proximal dendrites in neurons, and around vimentin bundles in ARSACS fibroblasts [25,29,55]. Additionally, neuronal differentiated SH-SY5Y sacsin KO cells exhibit fewer and shorter neurites, with decreased movement and number of mitochondria [24]. Together, these results illustrate a direct role of sacsin in cytoskeletal dynamics and organization, which impact protein and organelle transport.

#### Sacsin's Role in Mitochondria

Another characteristic of the lack of sacsin expression is the formation of elongated/hyperfused mitochondria, which suggests that sacsin is involved in the regulation of mitochondrial dynamics as well. In the absence of sacsin, a hyperfused, overly interconnected, and functionally impaired mitochondrial network is observed. In sacsin-deficient neurons, mitochondria mislocalize to the soma and proximal dendrites and have an abnormal balloon-like or bulbed morphology [25]. Sacsin localizes to mitochondria in non-neuronal cells and primary neurons and interacts with dynamin-related protein 1 (Drp1) [25,56]. How sacsin regulates mitochondrial morphology is unknown but it is likely that Sacsin-Drp1 interaction plays a role.

In addition to abnormal mitochondrial localization and morphology, mitochondrial function is also impacted, indicated by a decrease in mitochondrial membrane potential in sacsin knockdown neurons [25]. Additional evidence of abnormal mitochondrial functions are shown by microarray analysis and identification of altered transcript levels for oxidative phosphorylation

and oxidative stress genes, leading to decreased mitochondrial respiration and production of reactive oxygen species (ROS) in sacsin knockdown cells and ARSACS patients' fibroblasts [56]. This observation was confirmed using RNA-sequencing analysis to generate a whole-genome molecular signature profile of sacsin knockout cells [24]. Scavenging ROS with the mitochondrial-targeted antioxidant ubiquinone, MitoQ, protects Purkinje neurons in *Sacs-/-* mice against neurodegeneration [57]. Taken together, these results illustrate a direct role of sacsin in the localization, morphology, and function of mitochondria, which could impact neuronal functions and play a role in the abnormal synaptic input and intrinsic firing properties of ARSACS mice Purkinje neurons [28].

#### Sacsin Role in Autophagy

Autophagy is a sequential process characterized by the formation of P62-positive phagophores, then LC3 positive-autophagosomes, followed by fusion of autophagosomes with lysosomes forming the autophagolysosome, ending the degradation and recycling of proteins. Sacsin's role in autophagy was first described by Duncan et al. when they investigated the effect of the altered organization of intermediate filaments in ARSACS patients' fibroblasts [23]. The abnormal perinuclear accumulation of vimentin filaments contained mislocalized proteins associated with autophagy, namely, HSP70, ubiquitin, lysosome-associated membrane protein 2 (Lamp2), and sequestosome 1 (also known as ubiquitin-binding protein p62/SQSTM1), which suggest a role of sacsin in the regulation of autophagy [23]. Autophagic flux rate in ARSACS cells is still under debate. An increase in autophagic flux was shown in ARSACS fibroblasts under starvation conditions, as suggested by increased expression levels of Lamp2 and decreased expression levels of p62 [23]. Yet, levels of ubiquitinated proteins were unchanged. In contrast, Morani et al. documented an impaired autophagic flux in sacsin knockout cells. Inhibition of fusion

of autophagosomes with lysosomes in sacsin KO cells treated with bafilomycin A1 resulted in P62-Phagophore formation and absence of LC3 positive-autophagosome formation [24]. Absence of sacsin also reduced co-immunolocalization of LC3 with lysosomal and mitochondrial markers suggesting the inhibition of fusion of autophagic compartments and subsequent failed cargo degradation, particularly damaged mitochondria [24]. To reinforce the role of sacsin in autophagy, sacsin was recently found to control lysosomal positioning and reformation by regulating MT dynamics [22]. These findings suggest that sacsin regulates multiple steps involved in autophagy, and its absence dysregulates autophagic flux. However, the exact role of sacsin in the regulation of autophagy is still poorly understood, and further investigation is required to elucidate the precise regulatory mechanism.

#### **Sacsin Role in Protein Transport**

Romano et al. conducted a multi-omic profiling study in sacsin knockout cells to further the understanding of sacsin roles in regulating cytoskeletal organization, MT dynamics, and protein trafficking. They identified multiple mislocalized proteins in sacsin-deficient conditions after comparing proteomic and surfaceome datasets suggesting that sacsin plays a role in protein trafficking to or from the membrane [29]. Membrane-bound (vesicle) trafficking was also affected in sacsin knockout cells; fibronectin, a secreted protein, which is packaged into vesicles at the ER and Golgi and trafficked to the cell periphery along MTs, was retained in the ER in HEK293 and SH-SY5Y sacsin knockout cells suggesting a role of sacsin in vesicle trafficking. Similarly, integrin subunit alpha 1 (ITGA1), a plasma membrane cell-cell adhesion molecule, is abnormally accumulated in the soma of *Sacs-/-* cells and proximal dendritic trunks of Purkinje neurons and deep cerebellar nuclei (DCN) neurons, with decreased localization in axon tracts suggesting a role of sacsin in its transport and subcellular localization. Taken together, these findings suggest a role

of sacsin in protein transport and essential interactions with proteins involved in vesicle trafficking, such as Rabs.

# **Role of RAB1 in the Secretory Pathway**

Using a pulldown assay to demonstrate the interaction of SacsJ with IF proteins, we identified the SacsJ interactome and shed light to the interaction of sacsin J-domain with new partners, in particular, Rab1b, a member of the RAB family involved in the secretory pathway [58]. The two mammalian RAB1 isoforms, Rab1a (205aa) and Rab1b (201aa) bear 92% identical amino acids and are predominantly located at the membranes of the ER and Golgi apparatus but, have also been detected on autophagosomes and lipid rafts [59,60,61,62].

#### **Secretory Pathway General Overview**

The secretory pathway is responsible for synthesizing, folding, and delivering a diverse array of cellular proteins. It consists of the ER, the endoplasmic reticulum-Golgi intermediate compartment (ERGIC), the Golgi apparatus, and transport vesicles that traffic between these compartments [63]. The ER is the largest organelle of the cell and is the primary site of protein biosynthesis; it is composed of a rough ER, called such because of the presence of ribosomes which participate in protein biosynthesis, and the smooth ER, where ER exit sites (ERES) locate. Newly synthesized proteins exit the smooth ER and are transported to the ERGIC. The ERGIC is a vesicular structure located between the ER and Golgi apparatus that regulates vesicle trafficking between the two organelles [64]. The Golgi apparatus comprises polarized flattened sacs, called cisternae, responsible for transporting, adding post-translational modifications, and packaging proteins for delivery to downstream targets. Proper Golgi functionality requires an intact architecture; modifications in its structure have been shown to impact normal function and posttranslational modifications in mammalian cells [65]. The anterograde (ER to Golgi) and

retrograde (Golgi to ER) transport of cargoes between the ER, ERGIC, and Golgi involves two key steps: vesicle-budding from ER or Golgi membrane and subsequent tethering and fusion of vesicle to the target membrane. These events are highly dynamic and involve RAB proteins, which are master regulators of membrane trafficking in the secretory pathway.

#### RAB Protein Family and Molecular Mechanism Functions in Secretory Pathway Trafficking

In eukaryotic cells, Rab proteins regulate temporal and spatial trafficking activities between secretory pathway compartments. First identified in nervous tissue as a critical player of dendritic and axonal organization, RABs were shown to be crucial for vesicular transport and exocytosis of neuromediators during synaptic transmission [66]. The RAB proteins are low molecular mass monomeric GTPases, members of the Ras superfamily, and are coded by more than 60 genes in humans [67]. The classic structural organization of RAB proteins consists of a short N-terminal sequence made of a conserved "G box" essential for guanine nucleotide binding, a guanosine 5'-GTP hydrolysis domain, and a carboxyl (C)-terminal motif "CC motif" containing two conserved cysteine residues on which post-translational modifications, such as geranylgeranylation, allow membrane insertion. Rabs are synthesized in their inactive Rab-GDP bound form when first in the cytosol. Rab escort proteins (REP) will recognize these cytosolic free-floating Rabs and present them to geranylgeranyl transferase (GGT), which will attach covalently a geranylgeranyl post-translation motif to facilitate membrane anchoring for proteins. Membrane association of Rab is complex and extremely regulated. The geranylgeranylated Rab-GDP is escorted to the target membrane by REP and recognized by Rab GDP dissociation inhibitor (GDI), generating GDI-Rab-GDP, which is known to regulate the membrane cycle of the Rab proteins and keeps Rab-GDP in soluble cytosolic form. GDI physically masks the isoprenyl anchor allowing GDI-Rab-GDP to interact with the membrane-bound GDI displacement factor (GDF).

This interaction dissociates the GDI-Rab complex allowing the targeting of Rab-GDP to the membrane of organelles. The now membrane-bound Rab-GDP can interact with guanine nucleotide exchange factors (GEF) which catalyze a conformational change from inactive Rab-GDP to active Rab-GTP. Multiple effector proteins will recognize active Rab-GTP and serve their function in membrane trafficking. Lastly, specific GTPase-activating proteins (GAP) will inactivate Rab-GTP by accelerating the hydrolysis of the bound GTP to GDP while anchored at the organelle's membrane after completing the task. The inactive Rab-GDP can then be extracted from the membrane by GDI and recycled for another round of function [68].

#### PTMs and Regulation of Rab Activity

Regulation of Rab activity, localization, and function depends on its association with GDI, GEF, and GAP. However, PTMs such as prenylation, adenylylation, phosphocholination, phosphorylation, and ubiquitination also modify Rab functions. For example, prenylation of Rab in the form of the covalent addition of geranylgeranyl moities, reinforce Rab membrane anchorage and subcellular localisation [69,70]. Rab variants inhibiting geranylgeranylation are mistargeted to the ER or Golgi region rather than their originally designated cellular compartment [71]. Adenylylation, or AMPylation, is the covalent attachment of an adenosine monophosphate to tyrosine or threonine and is used by *Legionella pneumophila* to manipulate the host signal and promote infection [72]. AMPylated Rab1b stays in the GTP-bound state, restricting the access of GAPs, and target Rab1 to *Legionella*-containing vacuole to modulate virulence and replication of *Legionella pneumophila* [73]. Phosphorylation also mediates functional regulation and localization of Rab GTPases. Lai et al. reported that phosphorylation of Rab8 limits its GEF-mediated activation. Rab3a, Rab8a, and Rab10 were identified as substrates of Leucine-rich repeat kinase 2 (LRRK2) kinase responsible of inherited PD, which reduce their affinity to regulatory

proteins like GDI, and results in altered membrane to cytoplasmic pool distribution of these Rabs [74]. Phosphorylation is also specific to subcellular localization for Rab4p and Rab1Ap, predominately cytosolic or membranous, respectively [75]. Regarding Rab1, Levin et al. demonstrated that Transforming Growth Factor-β (TGF-β)-activated Kinase 1 (TAK1) phosphorylates Rab1 and inhibits its interaction with GDI, but not with GEF or GAP enzymes. Phosphorylated Rab1 is exclusively localized to membranes, suggesting that phosphorylation may promote Rab1 membrane insertion [76]. Lastly, ubiquitination can regulate Rab stability, activity, and localization. Ubiquitination may regulate Rab GTPase activity through two modes: the recruitment of effectors, and subcellular localization, where inactive GDP-bound forms are usually in the cytosol and active GTP—bound forms on membranes [77]. For example, the early endosome marker Rab5 is crucial in endocytosis and membrane transport, and its ubiquitination alters its activity in a residue-dependent manner. Monoubiquitylation of Lys140 impairs the interaction between Rab5 and its downstream effectors, and monoubiquitylation of Lys165 hinders GEFmediated nucleotide conversion suppressing its activity [78]. Ubiquitination of Rab7 also regulates its activity and localization; ubiquitination on Lys191 residue can inhibit the recycling from late endosomes to TGN (Trans Golgi Network), and polyubiquitination on Lys38 residue by the E3 ligase Parkin exhibits stronger affinity for its receptor Rab interaction Lysosomal protein (RILP), improving the activity of Rab7 and membrane localization [79]. Additionally, the dysregulation of Rab7 ubiquitination in Parkin-deficient cells leads to increased secretion of exosomes, a phenomenon observed in Parkinson's Disease (PD) [80]. Together, these studies demonstrate the crucial roles of PTMs in the modification and regulation of Rab function, activity, and localization in the secretory pathway, but nothing is known on Rab1 ubiquitinylation.

#### **RAB 1 Functions in Secretory Pathway Trafficking**

Rabs are master regulators of membrane trafficking because they function as molecular switches allowing membrane fusion upon the hydrolysis of GTP interacting with various effector proteins, such as in the secretory pathway [77]. Rab1 is implicated in ER-Golgi trafficking and plays a role in autophagy regulation. Rab1 localizes at ERES, vesicular tubular clusters (VTCs, at ERGIC), and Golgi membrane, where it interacts with organelle-specific effector proteins [59,81,82]. In particular, Rab1 associates with coat protein complex 1 (COPI) and 2 (COPII), soluble N-ethylmaleimide-sensitive factor attachment protein receptors (SNARE) complex, all Golgi membrane proteins, and with autophagy-related protein 9A (ATG9) to fulfill functions in protein trafficking and regulation of autophagy disrupted in ARSACS [83,84,85].

Rab1 is a critical protein in ER-Golgi vesicle transport by participating in cargo selection, vesicle fission, transport, tethering, and fusion to target membranes. For vesicle fission and cargo selection, Rab1 modulates both COPII and COPI membrane association-dissociation dynamics and sorting activity at the ER and Golgi, respectively [86,87,88]. After fission, Rab1 escorts the protein-containing vesicle and interacts with tethering and fusion Golgi membrane-related proteins, general vesicular transport factor p115 (p115), Golgi matrix protein (GM130), and Giantin [88,89,90]. Combined, they form a Rab1-dependent cis-SNARE complex allowing fusion of the vesicle to the target membrane and protein delivery [89,91]. The interaction between Rab1 and Golgi-morphology-forming proteins P115, GM130, and Giantin play a role in Golgi apparatus structural maintenance and morphology, and Rab1 expression levels alter Golgi morphology. For example, the transfection of Rab1bN121I blocked the forward transport of cargo and caused Golgi disruption into smaller vesicles in HEK293T cells [92]. Furthermore, overexpression of Rab1b modified Golgi size and gene expression in HeLa cells [93]. Together, Rab1 and its effectors play

a crucial role in the anterograde and retrograde transport of proteins and influence Golgi morphology and structure.

#### **Role of RAB1 in Autophagy**

Macroautophagy is a critical mechanism for the maintenance of cellular homeostasis. It does so by clearing and degrading damaged organelles and protein aggregates, recycling materials in stress conditions, and eliminating pathogens [94]. As shown by several authors, Rab1 plays a role in the formation and maturation of autophagosomes by recruiting proteins to the autophagosomes membrane and by regulating the activity of autophagy-related proteins [62,95,96,97]. Rab1b overexpression increases the number of autophagosomes in CHO cells, while Rab1 inhibition by transient overexpression of dominant negative Rab1bN121I decreased the number of autophagosomes and LC3-positive recruitment to membranes in different cell lines [62]. In fact, after autophagy initiation by starvation, Rab1 colocalizes with endogenous LC3, suggesting a role of Rab1 in the initial steps of autophagy [62]. The interaction of Rab1b with membrane associated ATG9A, responsible of membrane elongation of the autophagosome, suggests a role of Rab1 in membrane trafficking during autophagy [82,85,98,99].

#### **Involvement of Rab1 in Neurodegenerative Diseases**

In humans, autophagic dysfunction is a common feature of neurodegenerative disorders characterized by motor dysfunctions like PD and amyotrophic lateral sclerosis (ALS) [100,101]. Rab1 is directly linked to the development of PD and likely plays a role in other neurological diseases [102]. Rab1 suppresses alpha-Synuclein ( $\alpha$ -syn) toxicity and protects against mammalian dopaminergic neuronal death, which may point to a compensatory mechanism by the cell [103]. Overexpression of Rab1 reduces the accumulation of  $\alpha$ -syn by increasing ER-Golgi trafficking, disrupted by the aberrant interaction of  $\alpha$ -syn and GM130 [104]. Recently, a link between Rab1

and autophagy has been described for ALS and frontotemporal dementia (FTD). The Rab1a effector, C9orf72, was found to regulate the translocation of the Unc-51-like autophagy activating kinase (ULK) complex, known to initiate autophagosome formation, in the early steps of autophagy. C9orf72 controls autophagy initiation by regulating the Rab1a-dependent trafficking of the ULK1 autophagy initiation complex to the phagophore [105]. Lastly, the loss of Rab1 GTPase activity is associated with ER stress and neurodegeneration in ALS, and Rab1 overexpression rescues inhibition of ER-Golgi transport induced by mTDP-43, mFUS, or mSOD1 [106]. In ARSACS, like PD, autophagic flux is dysregulated. These studies suggest restoring normal Rab1 expression may be an attractive therapeutic target for neurodegenerative diseases like ARSACS.

Taken together, Rab1 has roles in protein trafficking and autophagy, and its dysregulation is linked to the pathogenesis of neurodegenerative disorders such as PD, FTD, and ALS. Like Rab1, sacsin is also involved in protein trafficking and autophagy, which are dysregulated in ARSACS. Consequently, Rab1 function is likely to be altered in the absence of sacsin, and critical interactions between Rab1 and sacsin remain to be discovered in the pathogenesis of ARSACS.

# Section 3: Rationale, Hypothesis, and Specific Aims

ARSACS is the second most prevalent form of ataxia in the world and there are currently no effective treatments to complement for the lack of sacsin. Our lab has demonstrated that the SacsJ domain targets and resolves pathological IF bundles seen in ARSACS. Generating cell penetrating peptide-fused to SacsJ, I demonstrated that IFs are clients of the J domain of sacsin [107]. Since J domain proteins often have multiple clients [108], we aimed to identify these other clients using a pulldown assay, amongst which RAB1 was found to be the second most abundant interacting partner. RAB1 is a master regulator of membrane trafficking between the ER and the

Golgi, which suggests a role of sacsin in membrane trafficking and in the secretory pathway. In particular, RAB1 cycles between the ER and Golgi and contributes to the anterograde transport of ER–produced proteins. I aimed to shed light on the function of the J-domain of sacsin in the regulation of ER-Golgi trafficking through its interaction with RAB1 and uncover new functions of sacsin in cellular trafficking.

# **Specific aims:**

- 1. To characterize the dose and temporal effect of a TAT-SacsJ peptide treatment on IF network in ARSACS cellular models (human derived-fibroblasts and murine motor neurons).
- 2. To identify interactors of the SacsJ domain and to determine if their expression is dysregulated in ARSACS cellular and mouse models.
- 3. To characterize the role of RAB1 and effect of lack of sacsin on secretory pathway organelle (ER, ERGIC, Golgi and autophagy) distribution and to determine if SacsJ or other sacsin domains could restore Rab1 subcellular localization.

#### **Section 4: Methods**

Cell culture and histology in mouse spinal cord

#### Fibroblasts and SW13- cells

Human skin fibroblasts control MCH74 were from the Cell Bank Repository for Mutant Human Cell Strains (McGill University Health Complex, Montreal, QC, Canada). ARSACS patient fibroblasts carrying the homozygous 8844delT mutation were previously described [25]. Immortalized fibroblasts were cultured in Dulbecco's Modified Essential Medium (DMEM) with 5-10% fetal bovine serum (FBS). Cultures were treated with GST-myc-TAT or GST-SacsJ-myc-TAT to assess the time-dependence (30 min to 24h) and dose-dependence (0-5 µM) of the

peptides' effect on the vimentin IF network, visualized by immunolabeling with antibody to vimentin (clone V9, MA5-11883 Thermofisher). Peptides were identified by immunolabeling using an anti-myc antibody (C3956, Sigma-Aldrich). Cy2 or Cy3 conjugated donkey secondary IgG antibodies against mouse or rabbit were from Jackson ImmunoResearch (1:300). Wild-type human adrenocarcinoma lacking endogenous intermediate filament expression (SW13vim-/-abbreviated to SW13-) and Sacs+/+ cells were cultured as previously described [109]. SW13-cells lacking sacsin expression (SW13- Sacs-/-) were produced using the sacsin double nickase plasmid following the manufacturer's instructions (SantaCruz Biotechnology, cat. no. sc-404592-NIC).

#### **Murine Spinal cord**

Primary cultures of dissociated spinal cord-dorsal root ganglia (DRG) were prepared from E13 Sacs-/- mice (C57B16 background) and wild-type (Sacs+/+) of the same background. Generation and characterization of the Sacs-/- mice were as described previously [27]. Cells were plated on glass coverslips (Fisher, ON, Toronto, Canada) coated with poly-D-lysine (P7280, Sigma-Aldrich) and Matrigel® (CACB354234, VWR, Town of Mount Royal, QC, Canada) and maintained in Eagle's Minimum Essential Medium (EMEM) enriched with 5 g/l glucose and supplemented with 3% horse serum, and other growth factors as previously described [110]. Cultures were used 6 weeks following plating to allow neuronal maturation and appearance of NF bundles in more than 80% of Sacs-/- MNs. Neurofilament bundles were defined as previously by a continuous filament bundle crossing the cell body from dendrite to dendrite [2] and labeled by indirect immunofluorescence with anti-NFL (clone NR4, N5139, Sigma-Aldrich). Paraformaldehyde-fixed brain and spinal cord of 7 months-old Sacs+/+ and Sacs-/- mice ere processed at the Histopathology - Research Institute of the McGill University Health Centre - RI-

<u>MUHC (rimuhc.ca)</u> for paraffin embedding and sectioning. The sections were then deparaffinized to carry out indirect immunofluorescence labelling.

#### Plasmid encoding Rab1

Because motor neurons (MN) in long-term primary spinal cord cultures are not transfectable, plasmids encoding Rab1bN121I was expressed by intranuclear microinjection of pcRab1bN121I or treated with 10µM brefeldin A (BFA; Sigma-Aldrich) for 30 minutes in *Sacs*—/— MN in culture as described in [111]. Twenty-four hours after injection, indirect immunofluorescence double labelling with antibodies against NFL and GM130 was performed, and the number of Golgi fragments were counted to assess Golgi morphology.

#### **Antibodies**

Primary antibodies used were: mouse monoclonal anti-NFL antibody clone NR4 (N5139, Sigma-Aldrich, 1:400), rabbit polyclonal anti-Rab1b (17824-1-AP, Protein Tech, 1:300), mouse monoclonal anti-KDEL (SPA-827, StressGen, 1:300), rabbit polyclonal anti-ATG9A (26276-1-AP, Proteintech, 1:300), rabbit polyclonal anti-GM130 (11308-1-AP, Proteintech, 1:300), rabbit polyclonal anti-ERGIC53 (13364-1ap, Protein tech, 1:300), mouse monoclonal anti-myc (A14, Santa Cruz Biotechnology, 1:400), and mouse monoclonal anti-GAPDH, (MM-0163-P, MediMabs, 1:1,000), mouse monoclonal anti-vimentin (V6639, Sigma 1:300), DAPI (1:1000), rabbit monoclonal anti-Sacsin (ab181190-100UL, Abcam1:1000)

Secondary antibodies: Peroxidase affinipure donkey anti-mouse and anti-rabbit IgG (715-035-150 and 711-035-152, 1:5,000), Cy2-conjugated (715-225-151, 1:300), Cy3-conjugated (715-165-151, 1:300) donkey anti-mouse IgG and Cy3-conjugated (705-165-147, 1:300) and donkey anti-goat IgG were from Jackson ImmunoResearch Laboratories (West Grove, PA, USA), 488-conjugated rabbit polyclonal (A-11034, Mol Probes, 1:300). Fluorescence microscopy: (Zeiss

Observer.Z1, ZenBlue 2.6 Software, 40x, McGill University) and spinning disk confocal microscopy (Olympus IX83 U-TBI90, Metamorph V.10 Software 100x, McBride Lab, McGill University) were used for visualization of fluorescent probes.

#### **Plasmids**

Plasmids encoding GFP-Rab1bwt or the dominant negative mutant Rab1bN121I were purchased from the MRC PPU reagent unit of University of Dundee (UK) cDNA Clone - Rab1b | MRC-PPU Reagents (dundee.ac.uk). Plasmids encoding sacsin myc-tagged domains of DNAJ, HSP40-binding-incompetent HSP70 carrying the H33Q variant DNAJ-H33Q (H33Q), UBL, SIRPT, and HEPN were produced by Norclone Biotech Laboratories, London, ON, Canada.\_C-terminus myc-tagged sacsin domains were constructed in pcDNA4.1(Norclone)) from pEGFP—sacsin full length (OriGene Technologies, Rockville, MD, USA): UBL (Sacs aa 1-84), SIRPT1 (Sacs aa 84-1374), SIRPT2 (Sacs aa 1444-2443), or SIRPT3 (Sacs aa 2512-4282), SacsJ (Sacs aa 4316-4420), and HEPN (Sacs aa 4422-4579).

#### **Transfection**

SW13- *Sacs*+/+ and SW13- *Sacs*-/- cells were plated in 24-well culture dishes and transfected when cells reached 90% confluence. Co-transfections of DNAJ, H33Q, UBL, SIRPT, HEPN, with GFP-Rab1bwt were transfected when cells reached 90% confluence and performed for 24-hours according to the manufacturers protocol using Lipofectamine 2000 (source).

#### **Recombinant protein production**

The SacsJ cDNA (corresponding to residues 4316-4420 of sacsin) was inserted in frame with GST into the pGEX6 vector using mouse pEGFP-sacsin full length (OriGene Technologies) as a template. For delivery into cells and tissues, the pGEX-SacsJ or GST were tagged on the C-terminus with a myc epitope to identify the peptide by anti-myc immunolabeling and with the

TAT-derived cell penetrating peptide sequence (YGRKKRRQRRR), which has been shown to confer efficient neuronal delivery and blood-brain barrier penetration [112]. All cloning was subcontracted. Plasmid carrying the SacsJ-myc-TAT or GST-myc-TAT cDNA were transformed into the Escherichia coli BL21 (DE3) pLysS for recombinant protein production. Bacterial cultures were grown overnight at 37 °C and then diluted at 1:100 (v/v) into 1L Luria–Bertani medium containing 100µg/ml ampicillin. Bacteria were grown at 37 °C with vigorous shaking at 225 rpm until they reach an OD600nm=0.6, recombinant protein expression was then induced using 1 mM isopropyl-1-thio-β-D galactopyranoside (IPTG) at 30°C for 4 hours. Bacteria were lysed in PBS buffer (137 mM NaCl, 2.7 mM KCl, 10 mM Na2HPO4, 2 mM KH2PO4 pH 7.4), supplemented with 1 mM phenylmethylsulfonyl fluoride (PMSF), 80 units of DNase,100 µg/ml lysozyme and Triton 0.1 %. After sonication, bacterial debris were pelleted using centrifugation. The supernatant was then filtered through a 0.2 µm filter and chromatography affinity purification of GST-myc-TAT or GST-SacsJ-myc-TAT using glutathione resin was carried out according to the manufacturer instructions.

#### **Pull down and Proteomic Analysis**

Two mg of mouse brain (cortex) were homogenized in Tris-buffered saline (TBS) (50 mM Tris-HCl, 150 mM NaCl, pH 7.5) with 1% Triton X100 and centrifuged 3 times to remove debris and insoluble proteins. The sample was then incubated with 2 mg of recombinant GST or with GST- SacsJ with 200 µl of Glutathione Sepharose resin for two hours at 4 °C and centrifuged for 30 seconds at 5000g at 4 °C. The supernatant was identified as the fraction containing non-binding proteins. Beads were washed 4–5 times with 1% Triton in TBS prior to sending to the (proteomic platform MUHC Proteomics Services - Research Institute of the McGill University Health Centre - RI-MUHC (rimuhc.ca), Montreal, Canada for MS/MS mass spectrometry to identify proteins.

Data were analyzed using the Scaffold software to identify binding partners of SacsJ domain versus a control GST, only proteins with more than two different peptides identified by mass spectrometry were considered as specific interacting partners. To determine the enrichment levels of common interactors of GST and DNAJ, quantitative analysis was performed using Scaffold software on 3 samples per condition followed by a statistical analysis using T-test. Protein interaction networks and biological processes in which the SacsJ domain is involved were identified using <u>STRING</u>: functional protein association networks (string-db.org).

#### Western blot

Protein samples were analyzed with 10-12% SDS-PAGE, and electrotransfered to nitrocellulose membranes (Merck Millipore, Cat ISEQ00010). Immunoblotting was carried out as follows: After blocking with 5% milk, the membranes were incubated with the following primary antibodies; rabbit anti-Rab1b antibody (1:1000) (Proteintech, Cat 17824-1-AP), rabbit anti-sacsin antibody (1:1000) (ABCAM, ab181190-100UL) at 4 °C for 12 h. The membranes were then incubated with horseradish peroxidase (HRP)-conjugated goat anti-rabbit IgG (Proteintech, Cat SA00001-2) secondary antibody (1:2500) for 2 h. Finally, the signal was detected using an enhanced chemiluminescence (ECL) (ThermoFisher Scientific, Pierce ECL Western Blotting Substrate, 32209X4) and images were acquired with INTAS (INTAS Science Imaging Instruments, GmbH Gustav-Bielefeld-Strasse 2 D-37079); GAPDH served as an internal control of protein loading.

## **Statistics IF organization**

Quantitative experiments are presented as mean  $\pm$  SD. The proportion of motor neurons or fibroblasts carrying a dismantled, regular or perinuclear IF network was quantified in at least 3 cultures per condition, with a minimum count of 30 cells per coverslip. The proportion of motor

neurons displaying a widely distributed or dendritic or somal-restricted organelle distribution was quantified in at least 3 coverslips per condition, with a minimum count of 30 motor neurons per coverslip. Statistical analysis was by one-way ANOVA followed by a Tuckey HSD post hoc analysis. P values < 0.05 were considered statistically significant.

## **Colocalization analysis**

Colocalization measurement is defined by the Pearson Correlation coefficient (PCC), which is a reliable and simple measure to evaluate fluorescent probe overlap and allows for further statistical analysis [113]. Rab1b colocalization with Golgi or ER was assessed following cotransfection of GFP-Rab1bwt and sacsin domains in SW13- Sacs+/+ and SW13- Sacs-/- cells, and visualized following indirect immunofluorescence double labelling with antibodies against myc epitope and GM130 or KDEL and confocal microscopy. PCC was measured by ZenBlue 2.6 colocalization software tool. Statistical analysis was performed by one-way ANOVA followed by a Tuckey HSD posthoc analysis to determine significance for colocalization coefficients. P values < 0.05 were considered statistically significant. Three individual coverslips for a total of 30 cells per condition were analyzed.

## **Section 5: Results**

Aim 1: To characterize the dose-response and temporal effect of a TAT-SacsJ peptide treatment on IF network in ARSACS cellular models.

A Cell-Permeant SacsJ Peptide captures the dynamics of Vimentin disassembly in Fibroblasts

First, we characterized the effect of SacsJ-myc-TAT peptide on the vimentin IF in immortalized MCH74 fibroblasts. Following dose-dependent SacsJ-myc-TAT peptide treatment,

both GST-myc-TAT and SacsJ-myc-TAT were detected in the cytoplasm, and to a lower degree in the nuclei of fibroblasts 30 minutes after treatment, indicating a proper internalization of our cell penetrating peptides (Fig. 1A). At 0.5 µM, SacsJ-TAT induces IF network reorganization shown by the appearance of a perinuclear vimentin ring in the majority of fibroblasts; this phenotype was barely observed in GST-myc-TAT or No Treatment conditions (1-2% of fibroblasts) (Fig. 1A-B). Higher SacsJ-myc-TAT concentrations induce a slight, but non-significant, increase in the perinuclear ring phenotype (Fig. 1B), suggesting that the kinetics of this ring formation had reached its maximum and/or was limited by an unknown factor.

Next, we characterized the effect of SacsJ-myc-TAT peptide on the IF vimentin network over time. While IF network in cells treated with GST-myc-TAT resembles untreated cells (Fig. 2A), in SacsJ-myc-TAT treated fibroblasts, the following phenotypes appeared in a time-dependent and stepwise process (Fig. 2A and 2B). First, perinuclear rings appeared at the 30-minute mark (Fig. 2B). Second, the dismantling vimentin network phenotype, described as short and non-continuous filaments of vimentin, appeared at 3h post-treatment and remained relatively constant over 24 hours (Fig. 2C). Third, the diffuse phenotype, described as a diffuse and barely detectable labeling of vimentin, appeared at the 12-hour mark, and increased at the 24-hour mark (Fig. 2D). Lastly, the juxtanuclear phenotype, described as the nascent agglomeration of vimentin in nuclear proximity, had a late onset and appeared at 24 hours post-treatment. In contrast to GST-myc-TAT, SacsJ-myc-TAT was barely detectable at 24h. This suggests clearance of our SacsJ-myc-TAT peptide and the juxtanuclear phenotype is likely reflecting a recovery stage (Fig. 2E).

Taken together, these results demonstrate that SacsJ-myc-TAT targets IF proteins leading to the stepwise disassembly of the IF network, reproducing our previous work using ectopic expression of the SacsJ domain by plasmid transfection [2].

### SacsJ Disassembles NF in Murine MNs in Culture

After observing disassembly of vimentin network by SacsJ-myc-TAT in MCH74 fibroblasts, we investigated the efficiency of SacsJ-myc-TAT in targeting the NF network in MN cultured from *Sacs-/-* mouse embryos in comparison to *Sacs+/+* MN spinal cord cultures (Fig. 3A). The TAT-SacsJ peptide dismantled the NF network in *Sacs+/+* MNs and significantly decreased NF bundles in *Sacs-/-* MNs demonstrating that SacsJ-myc-TAT effectively targets the NF network and resolves NF bundles (Fig. 4B). In contrast to the recovery phase of the vimentin IF network, the NF network do not pass through a stage of perinuclear ring after 30 minutes of SacsJ-myc-TAT treatment. All together, we have demonstrated that IF and NF are clients of the J domain of sacsin, and we have shown a difference in disassembly kinetics between vimentin and NF.

# Aim 2: To identify interactors of the SacsJ domain and to determine if their expression is dysregulated in ARSACS models

## Proteomic Analysis of the SacsJ Interactome Identifies a Role in Membrane Dynamics and Rab1b as a Most Abundant Binding Partner

Mass spectrometry analysis of a pulldown assay was used to identify SacsJ clients. We found IF proteins as well as novel binding partners (Fig. 5A and 5B). Comparison of proteins enriched by binding to either SacsJ or to the GST control are shown in a volcano plot. Statistically significant enriched or specific proteins are labeled as green squares or triangles. Rab1b from DNAJ sample is highlighted in yellow (Fig. 5C). List of interacting partners is displayed in the table of Fig. 5D, with most (top) enriched to least (bottom) enriched proteins. Consistent with previous data, IF were found in the interactome, which validates our approach. Next, the STRING interaction database was used to generate a map of protein-protein interactions and to analyze cellular processes involved with their functions (Fig. 5E). Analysis of Enrichment of Gene

Ontology identified the main cellular functions associated with this interactome. The analysis illustrates a role of SacsJ in different cellular processes, including regulating subcellular localization of organelles and protein (53%), Golgi and vesicle transport (19%), and in antigen processing and presentation of peptides (12%) (Fig. 5F). Amongst all the SacsJ clients, Rab1b was selected because it is the second most enriched protein and has functions in organelles dynamics and autophagy, which are disrupted in ARSACS.

Aim 3: To characterize the role of RAB1 and the effect of lack of sacsin on distribution of secretory pathway organelles (ER, ERGIC, Golgi and autophagy) and if SacsJ or other sacsin domains can restore Rab1 subcellular localization.

## Absence of Sacsin Upregulates Rab1b and Restricts its Distribution to the Cell Soma

To further explore the interaction between SacsJ and Rab1b, we first determined if the absence of sacsin had an impact on Rab1b expression and distribution. Western blot analysis comparing Sacs+/+ and Sacs-/- mouse spinal cord show an upregulation of Rab1b expression levels and the presence of additional bands migrating at higher molecular weights in the absence of sacsin expression, suggesting that sacsin regulates Rab1b and is implicated in post-translational modifications (Fig. 6A). Next, we assessed subcellular distribution of Rab1b in 6-month-old MNs of Sacs-/- and Sacs+/+ mouse spinal cord in situ by immunofluorescence. In Sacs+/+ MNs, Rab1b had an even distribution in the soma and the dendrites/cellular processes (Fig. 6B), whereas in Sacs-/- MNs, Rab1b was abnormally accumulated in the soma indicated by a higher fluorescence intensity and less immunofluorescence colocalized with NFL-positive dendrites and axons compared to wild-type. Our data suggests a functional interaction between sacsin and Rab1b in the regulation of Rab1b expression and subcellular distribution.

## Absence of Sacsin Restricts Distribution of Rab-1 related Organelles

We next studied Rab1b subcellular distribution in cultured MN and the consequence of lack of sacsin on Rab1b- dependent organelles. Fig. 7A schematic shows that Rab1b is a key small GTPase regulating membrane dynamics between ER-Golgi, the intermediate compartment ERGIC or the autophagic membranes labelled by ATG9. The distribution of Rab1b was assessed in MN of 6-week-old Sacs+/+ and Sacs-/- spinal cord cultures to compare to our mouse spinal cord findings and validate this cellular model. In Sacs+/+ MNs, Rab1b was widely distributed and present in the distal dendrites, whereas in Sacs-/- MNs, Rab1b was abnormally restricted to the soma and absent from distal dendrites, a similar pattern as observed in mouse spinal cord (Fig. 7B). While Rab1b-interacting organelles, ER, ERGIC, and Golgi are usually widely distributed and reach the extremities of distal dendrites in healthy MNs, they were restricted to the soma and absent in the distal dendrites in Sacs-/- MNs. This distribution pattern is similar to Rab1b (Fig. 7C-E). ATG9-positive autophagic membranes are usually found to be widely distributed in the soma and present in proximal dendrites of Sacs+/+ MNs (Fig. 7F); however, they were abnormally compacted in the soma in Sacs-/- MNs and ATG9 immunofluorescence intensity was higher, which is consistent with the previously defined role of sacsin in autophagy (Fig. 7F). ATG9 membranes are juxtaposed to NF bundles, which suggests that NF bundles are not degraded through autophagy but rather play a role in anchoring autophagosomes (Fig. 7G). The Golgi apparatus morphology and function relies on a balanced and constant trafficking of membranes and proteins regulated by Rab1b and we aimed to determine if the Rab1b and Golgi dynamics was conserved. First, Golgi compaction was observed in Sacs-/- MNs, characterized by fewer number of Golgi fragments compared to Sacs+/+. Inhibition of the association of Rab1 with the Golgi membrane by ectopically expressing the dominant negative mutant (Rab1N121I) severely

disrupted the Golgi apparatus in *Sacs-/-* MNs in culture (Fig. 8A), which indicates that the compaction of the Golgi apparatus is reversible. We confirmed these findings using Brefeldin A (BFA), which inhibits ER-Golgi transport by another small GTPase called ADP Ribosylation Factor 1. Taken together, these results demonstrate the role of Rab1b in the observed abnormal Golgi morphology and the reversibility of Golgi compaction observed in the absence of sacsin.

Yet, abnormal subcellular localization of this Rab1b-interacting organelle could be the result of physical displacement caused by the formation of NF bundles. As shown by immunofluorescence, NF bundles in *Sacs-/-* MNs in culture were highly compact, rigid, cable-like structures occupying the soma which could result in physical interactions and displacement of the Golgi apparatus and/or affect its morphology (Fig. 9A). These NF bundles observed by electron microscopy show the eccentric position of the Golgi in *Sacs-/-* MNs in culture (Fig. 9B, right panel), raising the question of whether the organellar abnormalities are secondary to the formation of NF/IF bundles.

## Rab1b and Organelles Abnormalities are Direct Targets of Sacsin

To determine if NF/IF bundles have an impact on the Golgi apparatus, we next used Adrenocarcinoma SW13- cells lacking endogenous intermediate filaments. SW13- *Sacs-/-* cells are knocked out for sacsin and SW13- *Sacs+/+* cells serve as a control. Like in *Sacs-/-* MNs, Rab1b was upregulated and extra bands of higher molecular weight were seen on Western blots indicative of post-translational modifications in SW13- *Sacs-/-* cells (Fig. 10A). Abnormalities in Golgi morphology (i.e.; compaction and restriction of subcellular localization of the Golgi in absence of sacsin) also occurred in SW13- *Sacs-/--* (Fig. 10B). All together, these results validate the SW13- *Sacs-/-* as a model of ARSACS and show that the lack of IF does not affect either Rab1b upregulation and abnormal post-translational modifications or abnormal Golgi compaction.

## Sacsin Domains Alter Rab1b Subcellular Distribution and Association with ER in SW13-Sacs-/- Cells

Because compaction of the Golgi could result from unbalanced Rab1b association to the Golgi, we next used SW13- cells to determine the role of sacsin on Rab1b subcellular localization without the interference of IF bundling. First, Rab1b association with Golgi or ER was characterized by measuring the Pearson Colocalization Coefficient (PCC) of GM130 or KDEL with ectopically expressed Rab1b-EGFP, allowing for direct observation of Rab1b, which avoids the possibility of artefacts due to antibody specificity. EGFP-Rab1b was generally enriched at the Golgi, like endogenous Rab1b, and was strongly co-localized with GM130 in SW13- Sacs+/+ and SW13- Sacs-/- cells (PCC values of 0.87 and 0.84, Fig. 11A). EGFP-Rab1b also localized to the ER membrane but to a lesser extent (PCC values of 0.25 and 0.28) (Fig. 12A). Expression of sacsin J domain and other sacsin domains did not significantly affect Rab1b localization with the Golgi apparatus in both SW13- Sacs+/+ and SW13- Sacs-/-cells (Fig. 11B-C). However, it did affect the localization of Rab1b in ER; expression of DNAJ, DNAJH33Q, and UBL sacsin domains significantly increased Rab1b association with the ER, while SIRPT1 and HEPN had no effect (Fig.12B-C). The data demonstrates that ER enrichment is not dependent on HSP70 binding, SIRPT1 or HEPN functions.

## **Conclusion and Contribution to Original Knowledge**

I characterized a cell-penetrating peptide, SacsJ-myc-TAT, and tested its efficiency in modifying the IF/NF network in fibroblasts and MNs; treatment with this peptide results in the stepwise dissolution of the IF network or bundles caused by the absence of sacsin expression. We next identified SacsJ clients and investigated the role of sacsin in the regulation of Rab1b functions. The absence of sacsin is associated with changes in Rab1b level and distribution; Rab1b was

upregulated, differences in posttranslational modifications were suggested, and subcellular distribution was altered. Organelles involving Rab1b present with an abnormal distribution in the absence of sacsin, which illustrates the role of sacsin through its interaction with Rab1 on ER, ERGIC, Golgi and ATG9-vesicle subcellular distribution. These abnormal organelle localizations and morphologies were independent of the presence of intermediate filaments, in particular of IF bundles. The expression of SacsJ domain, the SacsJH33Q variant lacking Hsp70 binding ability, and the UBL domain increased Rab1b colocalization with the ER in SW13- Sacs-/- cells. In SW13-Sacs+/+ cells, expression of sacsin domains did not impact Rab1b distribution to the Golgi or ER. These results suggest that multiple sacsin domains cooperatively regulate Rab1b functions and the secretory pathway. The question remains whether expression of an individual domain is sufficient to preserve function as well as distribution of the secretory pathway components.

## **Section 6: Discussion, Conclusion and Future Directions**

## **Summary of Main Findings**

Sacsin is a gigantic multidomain protein that regulates IF homeostasis [2]. In this study, we further the understanding of the role of the sacsin J domain in IF network dynamics and discover new functions by identifying novel clients of the J domain. By focusing on Rab1b, we illustrate new sacsin functions associated with membrane dynamics and shed light on the pathogenesis of ARSACS.

#### SacsJ and Intermediate Filaments

Our chimeric cell-penetrating peptide fused to the J domain of sacsin targets the IF network in both control and sacsin knockout fibroblasts and MNs, confirming our previous results that sacsin J domain is a crucial regulator of NF and vimentin IF network in cells [2]. Treatment with the SacsJ peptide led to the stepwise disassembly of the IF network in MCH74 control fibroblasts,

starting with the apparition of a perinuclear ring followed by the dismantling and dissolution of vimentin-labeled IF proteins, which is reminiscent of the role of Mrj, a DNAJ/HSP40 involved in disassembly of pre-existing keratin IF [114]. Similarly, treatment with SacsJ-TAT resulted in the dissolution of the NF network in wild-type cultured MNs and resolution of NF bundles in sacsin knockout MNs. The dissolution of the NF network in wild-type MNs is problematic; depletion of NFL protein has been shown to cause sensorimotor dysfunctions and spatial deficits in mice [115]. Therefore, on its own, SacsJ-TAT as a therapeutic agent is likely not a viable strategy. Nonetheless, these results confirm the role of SacsJ in IF network dynamics and join the ranks of the few HSPs regulating IF dynamics. Further studies in the laboratory are examining combinations of the SacsJ domain with other sacsin domains in modulating IF network.

## **Identification of SacsJ Clients**

We have identified interactors of the sacsin J domain that may shed light on the overall functions of sacsin. EndophillinA1 (SH3GL2), ARF5, RAB2A, RAB1b and HIP1R are SacsJ interactors with known roles in membrane dynamics. SH3GL2 is involved in membrane dynamics via the formation of endocytic vesicles and polymerization of actin around nascent vesicles [116]. ARF5, Rab2B and Rab1b are small GTPase involved in ER-Golgi trafficking, while HIP1R, another membrane-associated protein that interacts with huntingtin, regulates clathrin-dependent endocytosis, actin polymerization, and dendritic development and synapse formation [117,118]. On the other hand, the cytoplasmic FMR1 interacting protein (CYFIP1) binds to the RNA-binding protein FragileX Mental Retardation Protein to repress synaptic protein synthesis and to regulate actin polymerization [119,120]. All these key interacting partners point to a crucial role of sacsin in membrane dynamics.

We focused on Rab1b to explore the role of SacsJ in membrane dynamics because Rab1b is one of the major interactors of the sacsin J domain and is a master regulator of ER-Golgi membrane trafficking. The absence of sacsin led to increased expression levels of Rab1b and the apparition of higher molecular weight bands on Western blot analysis, suggesting that sacsin regulates PTMs on Rab1b. PTMs have been shown to regulate the activity, function, and localization of Rab1 [121]. In fact, Rab1b is abnormally localized in the soma and absent in the distal dendrites of sacsin knockout MNs, a distribution pattern reminiscent of ITGA1 in sacsin deficient neurons, which confirms the role of sacsin in protein localization and trafficking [29]. Rab1b interacting proteins and organelles are also mislocalized in absence of sacsin; the ATG9 protein, ER, ERGIC, and Golgi are concentrated in the soma and mostly absent from dendrites; a cellular distribution mirroring Rab1b. Similarly, mitochondria and lysosomes are also mislocalized in sacsin-deficient cells, reinforcing the role of sacsin in organelle distribution and suggesting a general function of sacsin in membrane dynamics possibly through the interaction with Rab1b and/or other Rabs [22,25]. It is likely that sacsin, via the J domain, regulates Rab1b PTMs and plays a role in the secretory pathway by affecting Rab1b subcellular distribution and function in membrane dynamics.

## Sacsin Regulate Golgi Morphology through Rab1b

We showed that alterations in organelle distribution and morphology are still present when IF bundles are removed, indicating that abnormal organelle subcellular distribution and morphology in cells lacking sacsin is not a consequence of physical displacement by IF bundles pointing to a direct effect of sacsin on Rab1b. Lack of sacsin causes a compaction of the Golgi, which is reminiscent of Rab1's role in regulating Golgi morphology. While downregulation of Rab1b induces Golgi apparatus fragmentation (Fig. 8A, [122]), overexpression leads to Golgi

enlargement [93]. We did observe an overexpression of Rab1b in the absence of sacsin; however, Golgi is rather compacted in *Sacs-/-* MNs and SW13- *Sacs-/-* cells. While the Golgi disruption is a common observation in neurological disease, the compaction of the Golgi has been observed in few conditions and is rather dependent of actin polymerization and Rab1 functions [123,124]. Indeed, Rab1b indirectly affects Golgi morphology through functional interaction with its known Golgi-morphology-forming effector proteins, including GM130, p115, GBF1, and Golgi phosphoprotein-3 (GOLPH3). GM130 maintains the ribbon structure of the Golgi complex, p115 is essential for the biogenesis of the Golgi apparatus, GBF1 maintains Golgi architecture, and GOLPH3 facilitates Golgi extension [89,92,125,126,127,128,129].

## Role of Sacsin Domains in the Regulation of Rab1b Functions

Rab1b localization to either the Golgi apparatus or ER is not different in sacsin knockout cells compared to wild-type. However, the transfection of plasmids encoding sacsin domains Dnaj, Dnaj<sup>H33Q</sup>, or Ubl increased Rab1b localization to the ER only in absence of sacsin, suggesting that these domains compensate only in the context of lack of sacsin and that sacsin can influence Rab1b subcellular localization. The fact that a similar ER enrichment is observed when Dnaj and the HSP70-binding-incompetent variant Dnaj<sup>H33Q</sup> are expressed indicates that this Rab1b-ER localization is not dependent on HSP70. Our data regarding the distinct roles of individual sacsin domains in the regulation of Rab1b subcellular localization indicates that they likely cooperate to regulate Rab1 functions, as observed previously for IF dynamics [2], and that expression of a specific domain of sacsin in a knockout context represent a snapshot of the function of this domain.

Considering that high molecular weight bands labeled by anti-Rab1b are present on Western blots in the absence of sacsin, the increased localization of Rab1b to the ER following expression of sacsin domains is likely a result in modification of PTMs on Rab1, more specifically,

phosphorylation or ubiquitinylation. Phosphorylation and ubiquitinylation are known regulators of cellular process, including autophagy, chaperone activity, and NF organization, which are all disrupted in ARSACS and implicate Rab1b [130,131].

Indeed, Levin et al. demonstrated that phosphorylation modified membrane/cytosolic localization of Rab1b, where phosphorylated-Rab1b exclusively localized to membranes. This suggests that Dnaj and Ubl may increase Rab1b phosphorylation and promote Rab1b association to ER membrane. Further studies will be required to identify the role of sacsin on PTMs, supported by the fact that phosphorylation has been shown to be affected in ARSACS. Indeed, lack of sacsin increases hypo-phosphorylated NFH in neurons and brain and Ataxin-2-like (ATX2L), a stress granule protein regulating IFN expression, while stathmin (STMN1), a microtubule scaffold, and ADP-ribosylation Factor Like GTPase 3 (ARL3), involved in cilia formation, are hyperphophorylated in ARSACS patient-derived fibroblasts [27,132,133].

Ubiquitinylation is a complex process leading to different effects on the same protein. For example, mono- and polyubiquitination, as well as residue-specific ubiquitinylation have different effects on the regulation of Rab activity, localization, and interaction with its effector proteins [121]. Ubiquitination was also shown to regulate the activity and localization of Rab5 and Rab7, both implicated in the endocytic pathway, by modifying their interaction with effector proteins and subcellular localization [79]. In fact, site specific monoubiquitination of Rab5 disrupts effector and guanine nucleotide binding, while subcellular fractionation indicates that RNF167 activity, a E3 ubiquitin-ligase protein, maintains Rab7's membrane localization and RNF167-mediated ubiquitination of Rab7 is impaired by variants of Charcot-Marie-Tooth Type 2B disease [78,134]. Although not reported before, it is possible that sacsin regulates ubiquitinylation of Rab1.

#### Conclusion

To summarize, we first developed a cell-penetrating peptide to study the direct effect of the sacsin J domain on NFs assembly and dynamics and, we confirmed the role of sacsin in regulating cytoskeletal dynamics. To further the understanding of the role of sacsin J domain, we identified its interactome and its role in membrane dynamics. We demonstrated that organelles affected by Rab1b are mislocalized in the absence of sacsin, confirming a functional interaction between Rab1b and Sacsin. In the absence of sacsin, Rab1 is overexpressed and shows an abnormal migration pattern on SDS-PAGE, which is reminiscent of PTM. Although the PTM(s) have not been identified yet, it is likely that they are regulated by the J domain of sacsin, which expression in SW13- Sacs-/- regulates Rab1b association to ER membrane. Altogether, our results show a role of sacsin in membrane dynamics by regulating Rab1b subcellular localization and functions.

## **Future Directions**

The next step to understand sacsin's role in protein regulation is to identify the additional post-translational modifications on Rab1b in absence of sacsin. These findings could reveal important aspects of the signaling regulating morphology and subcellular localization of organelles and provide a therapeutic approach targeting this mechanism of action, which is of particular interest for neurological disorders. In addition, how the different domains of sacsin cooperate to regulate these PTMs on Rab1b and their respective roles in regulating protein functions remain to be identified.

## **Section 7: Figures**

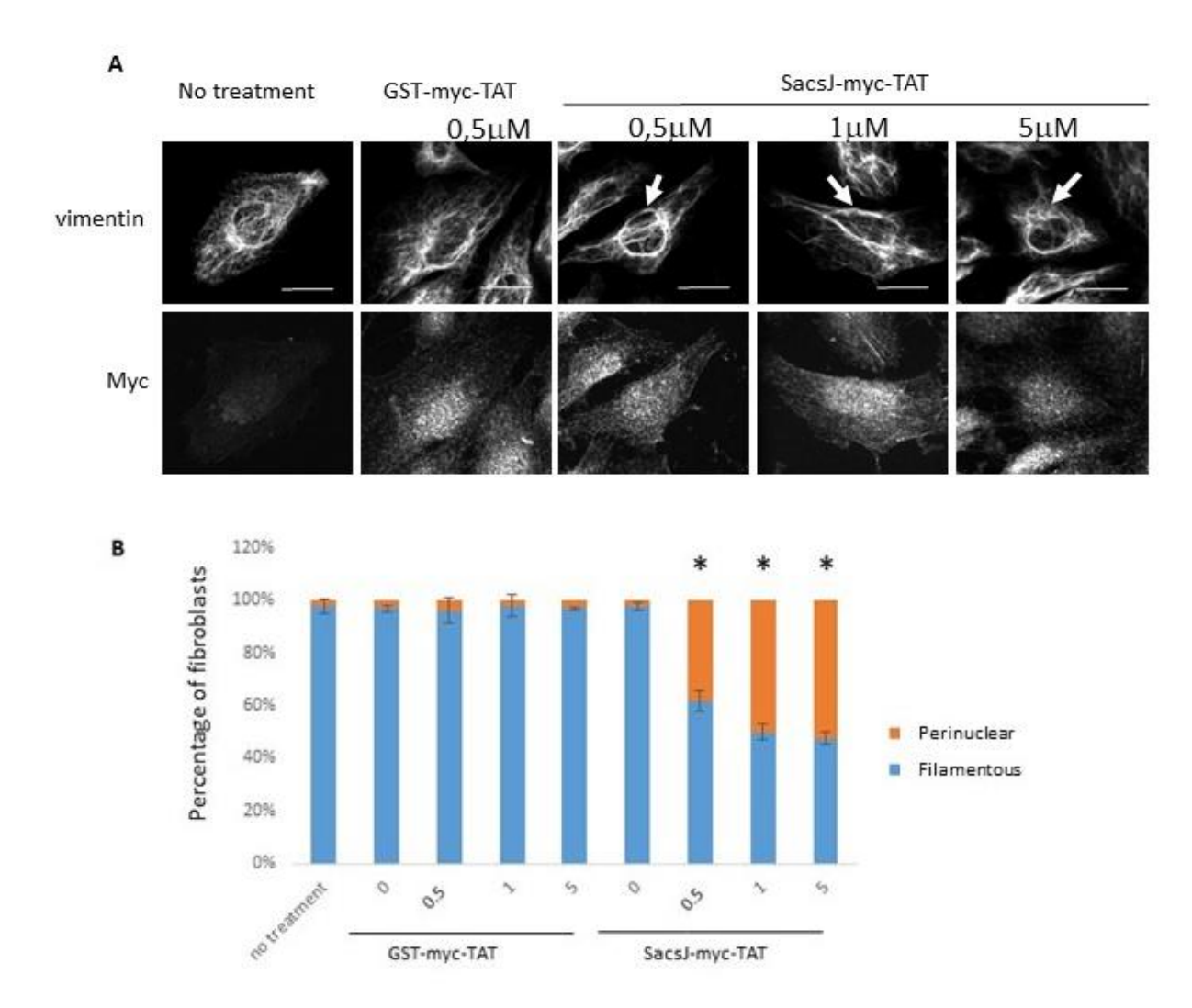


Figure 1. The cell-permeant peptide, SacsJ-myc-TAT, induced stepwise disruption of the vimentin IF network in MCH74 fibroblasts. A) Representative 3-dimensional reconstructions of Z-stack confocal images of MCH74 fibroblasts double labelled with anti-myc (rabbit anti-myc) and anti-vimentin (V9 mouse monoclonal) treated with increasing concentrations of Sacs-myc-TAT as indicated (0,5 to 5  $\mu$ M) or control peptide GST-myc-TAT. Treatment with SacsJ-myc-TAT for 30 min resulted in nuclear rings of bundled vimentin IF (large arrow). Scale bar: 20  $\mu$ m. B) Quantitation of the percentage of fibroblasts presenting circum-nuclear IF bundles or finely distributed IF when treated with increasing concentrations of SacsJ-myc-TAT (0,5 to 5  $\mu$ M) showing an increase in the percentage of cells with IF concentrated surrounding the nucleus. \*p< 0.05 vs NFL alone, one-way ANOVA (n=3). Note the diffuse distribution of labelling of the myc tag on SacsJ.

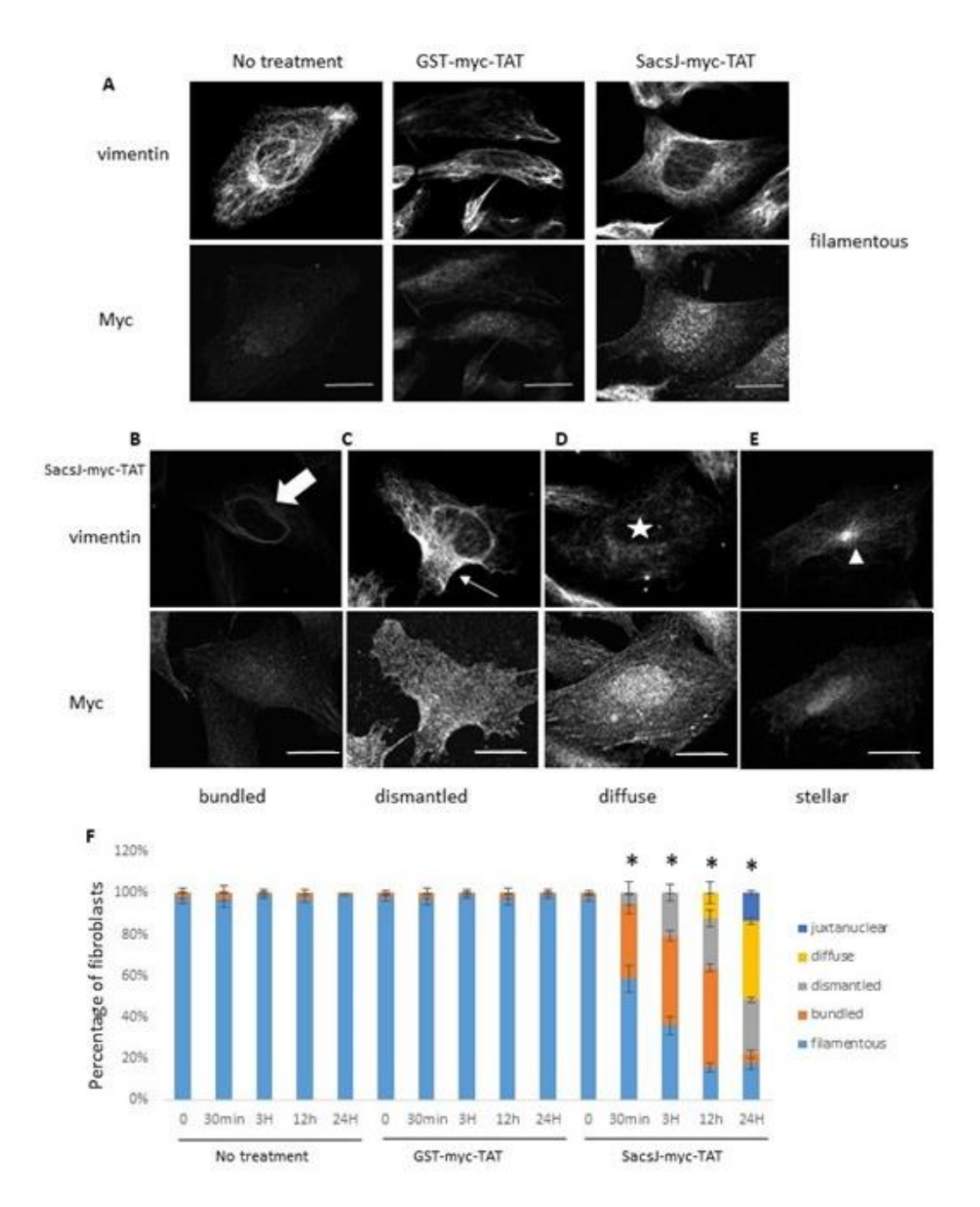
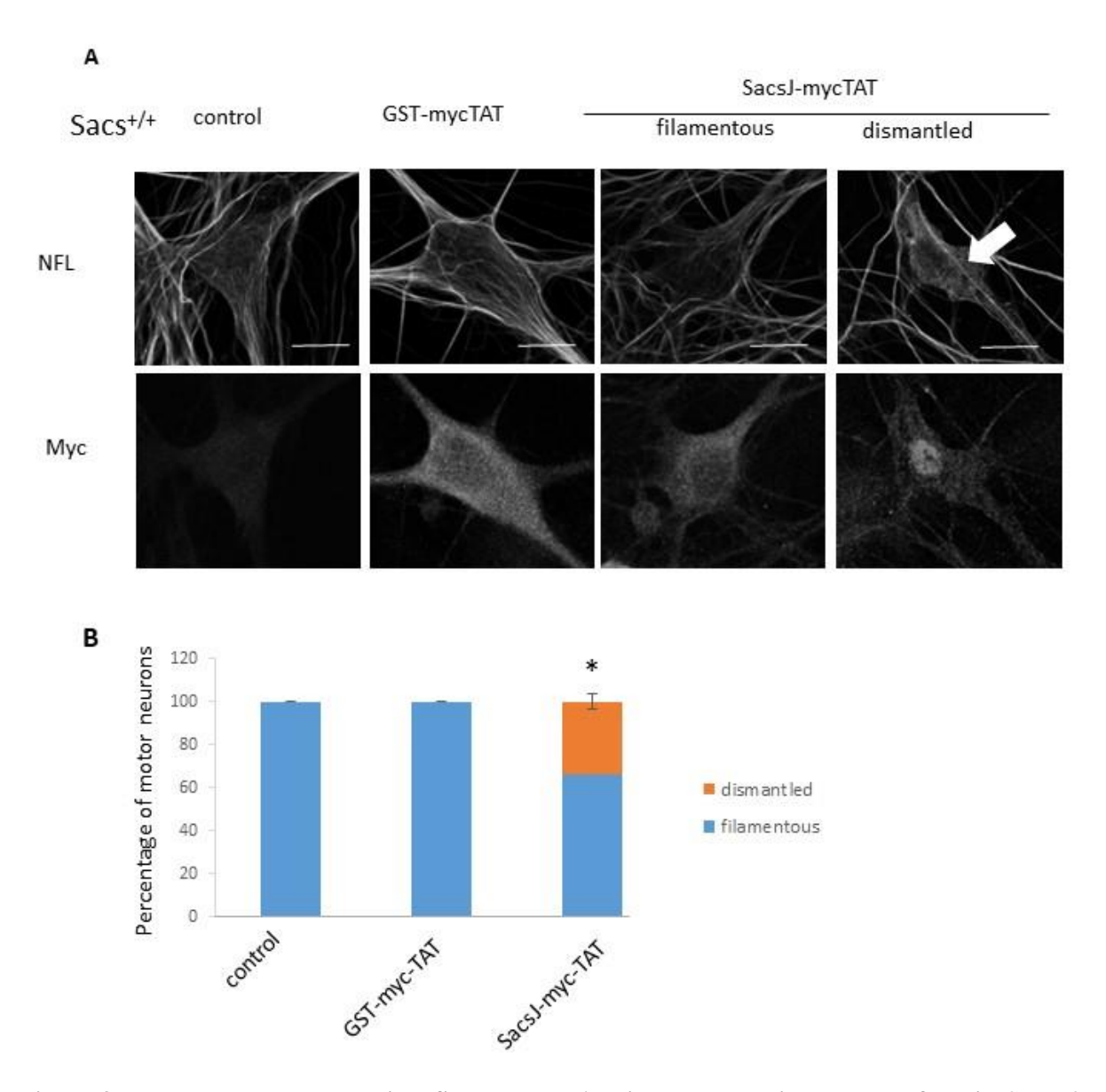


Figure 2. Over time, SacsJ-myc-TAT treatment resulted in the gradual disassembly of vimentin IF in MCH74 fibroblasts. A) Representative 3-dimensional reconstructions of Z-stack confocal images of fibroblasts double labelled with anti-myc (rabbit anti-myc) and anti-vimentin (V9 mouse monoclonal). Scale bar:  $20 \,\mu\text{m}$ . (B-E) MCH74 fibroblasts were treated with GST-myc-TAT control or SacsJ-myc-TAT (0,5  $\mu$ M) for 30 min, 3 h, 12 h or 24 h and showed time-dependent phenotypes: perinuclear rings of bundled vimentin (B, large arrow), dismantled vimentin network (C, small arrow), diffuse vimentin labelling (D, star), and appearance at a juxtanuclear accumulation (E, arrowhead). F) Quantitation of the percentage of fibroblasts presenting those phenotypes over duration of SacsJ-myc-TAT treatment. \*p< 0.05 vs time-matched no treatment or treated with GST-myc-TAT (0,5 $\mu$ M) one-way ANOVA, HSD Tuckey post hoc analysis (n=3).



**Figure 3.** The cell-permeant peptide, SacsJ-myc-TAT, induced the disassembly of NF in Sacs+/+ motor neurons in culture. A) Representative 3-dimensional reconstructions of Z-stack confocal images of double labelling with anti-myc (rabbit anti-myc) and anti-NFL (mouse anti-NFL) in Sacs+/+ 6-week-old murine spinal cord-DRG cultures showing the NF network and distribution of myc-TAT peptides in motor neurons. Cultures were treated with SacsJ-myc-TAT (0,5 μM) or GST-myc-TAT control peptide for 30 min and compared to untreated cultures. SacsJ-myc-TAT dismantled the endogenous NF network (large arrow). Scale bar: 20 μm. **B)** Quantitation of the percentage of motor neurons presenting a filamentous or dismantled NF network when treated with Sacs-mycTAT (0,5 μM). \*p< 0.05 vs no treatment or treated with GST-myc-TAT (0.5μM) using a one-way ANOVA, HSD Tuckey post hoc analysis (n=3).

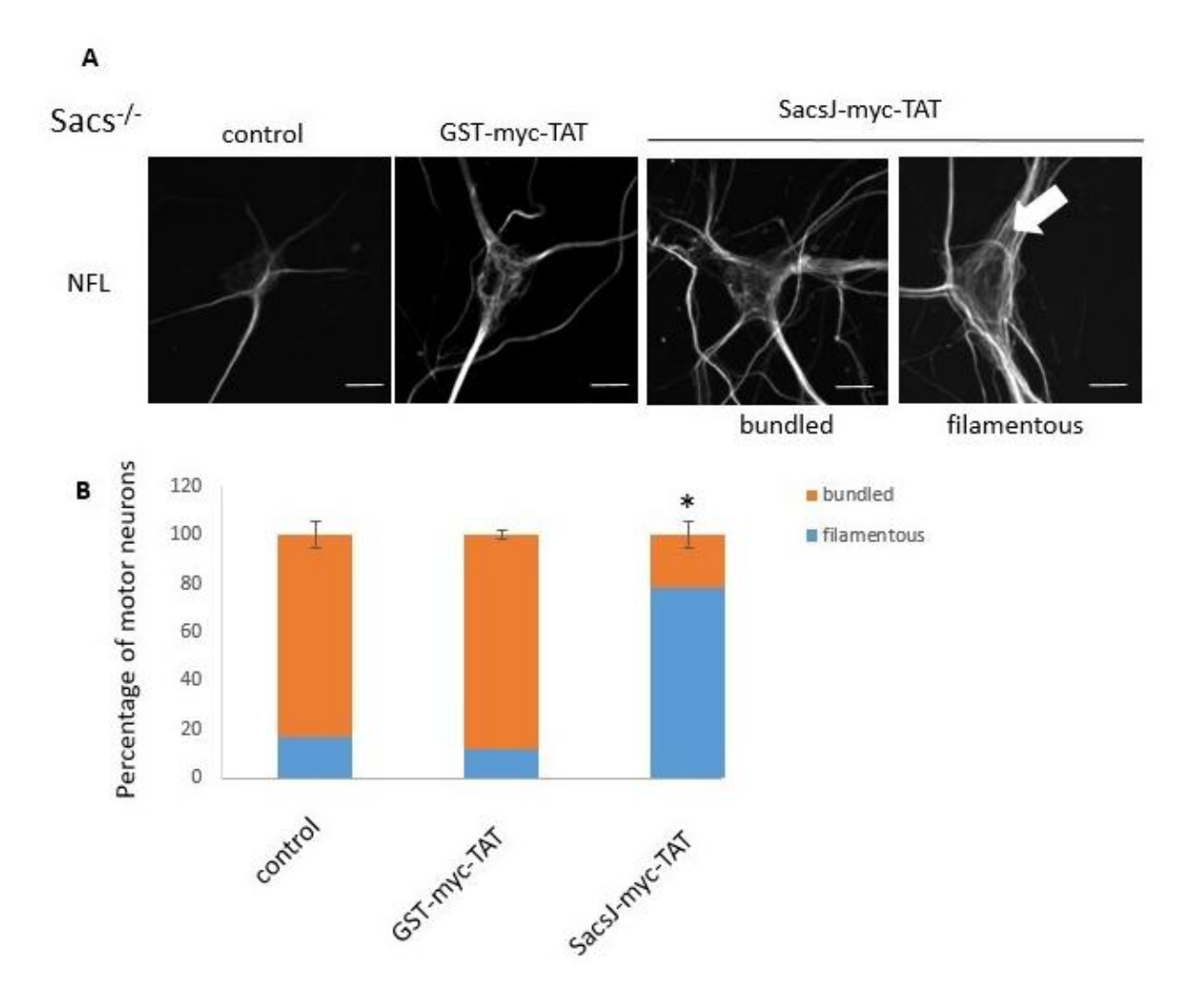
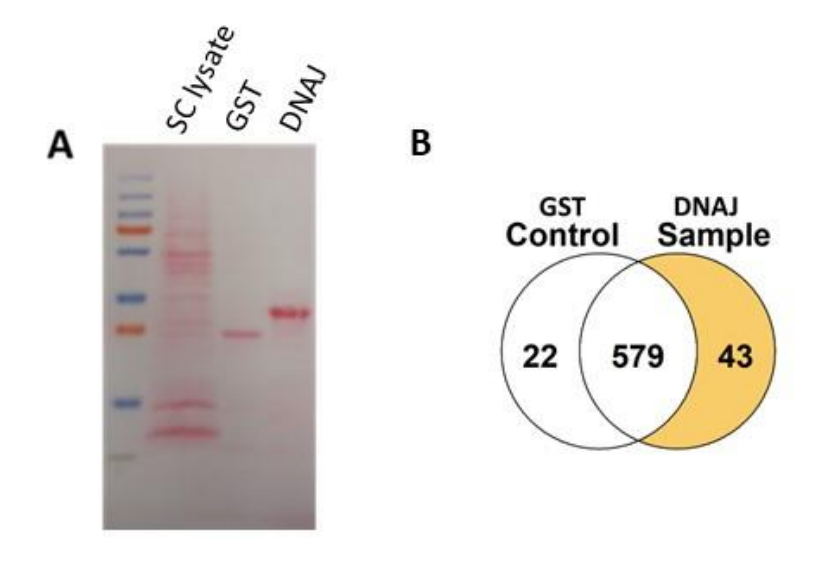
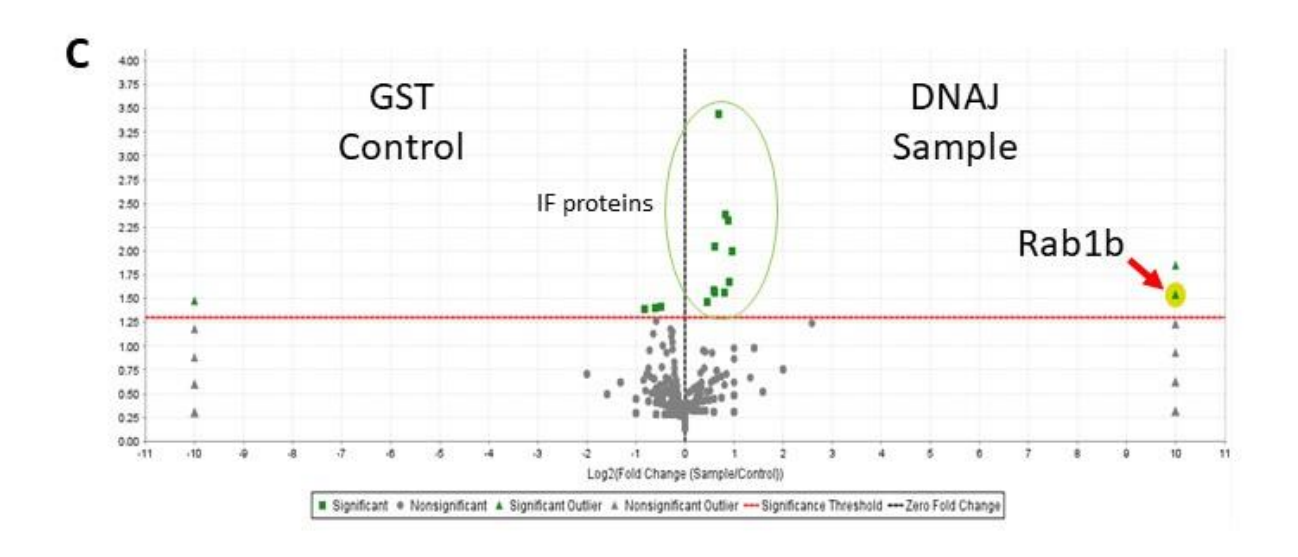


Figure 4. The cell-penetrating peptide, SacsJ-myc-TAT, resolved NF bundles in Sacs-/- motor neurons in culture. A) Representative 3-dimensional reconstructions of Z-stack confocal images of motor neurons in Sacs-/- 6-week-old spinal cord-DRG cultures double labelled with anti-myc (rabbit anti-myc) and anti-NFL (mouse anti-NFL) to show the NF network and SacsJ-myc-TAT distribution in motor neurons. Cultures were treated with SacsJ-myc-TAT (0,5  $\mu$ M) or GST-myc-TAT control peptide for 30 min and compared to untreated cultures. Treatment with SacsJ-myc-TAT resolved the NF bundles (large arrow). Scale bar: 20  $\mu$ m. B) Quantitation of the percentage of motor neurons presenting a filamentous or bundled NF network when treated with Sacs-myc-TAT (0,5 $\mu$ M). \*p< 0.05 vs no treatment or treated with GST-myc-TAT (0,5 $\mu$ M) using a one-way ANOVA, HSD Tuckey post hoc analysis (n=3).





Accession	Protein Name
SACS_MOUSE	Sacsin OS=Mus musculus GN=Sacs PE=1 SV=2
CYFP1_MOUSE	Cytoplasmic FMR1-interacting protein 1 OS=Mus musculus GN
RAB1B_MOUSE	Ras-related protein Rab-1B OS=Mus musculus GN=Rab1b PE=1.
ARFS_MOUSE	ADP-ribosylation factor 5 OS=Mus musculus GN=Arf5 PE=1 SV.
HIP1R_MOUSE	Huntingtin-interacting protein 1-related protein OS=Mus muscu.
DDX41_MOUSE	Probable ATP-dependent RNA helicase DDX41 OS=Mus muscul.
SH3G2_MOUSE	Endophilin-A1 OS=Mus musculus GN=Sh3gl2 PE=1 SV=2
DCTN2_MOUSE	Dynactin subunit 2 OS=Mus musculus GN=Dctn2 PE=1 SV=3
GDIB_MOUSE	Rab GDP dissociation inhibitor beta OS=Mus musculus GN=Gdi
RAB2A MOUSE	Ras-related protein Rab-2A OS=Mus musculus GN=Rab2a PE=1.

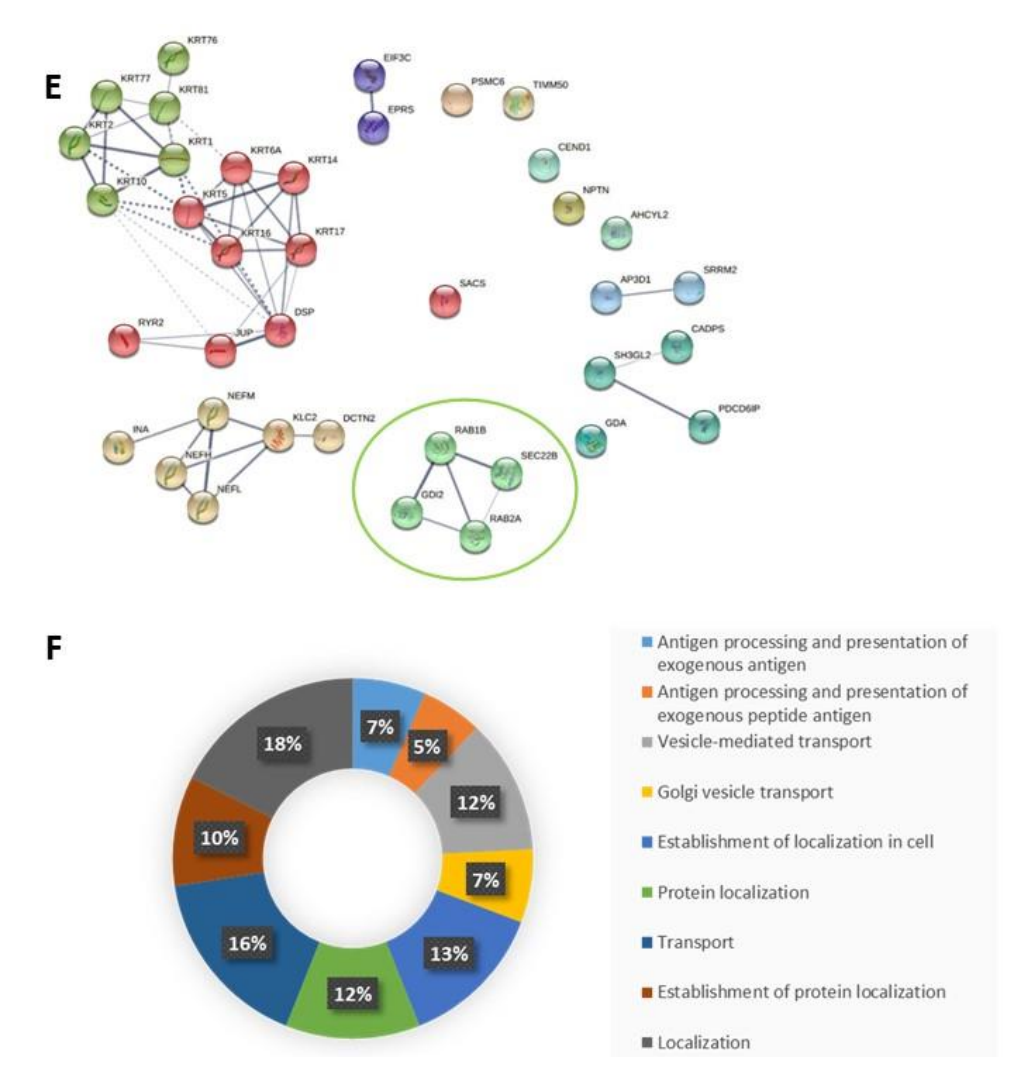
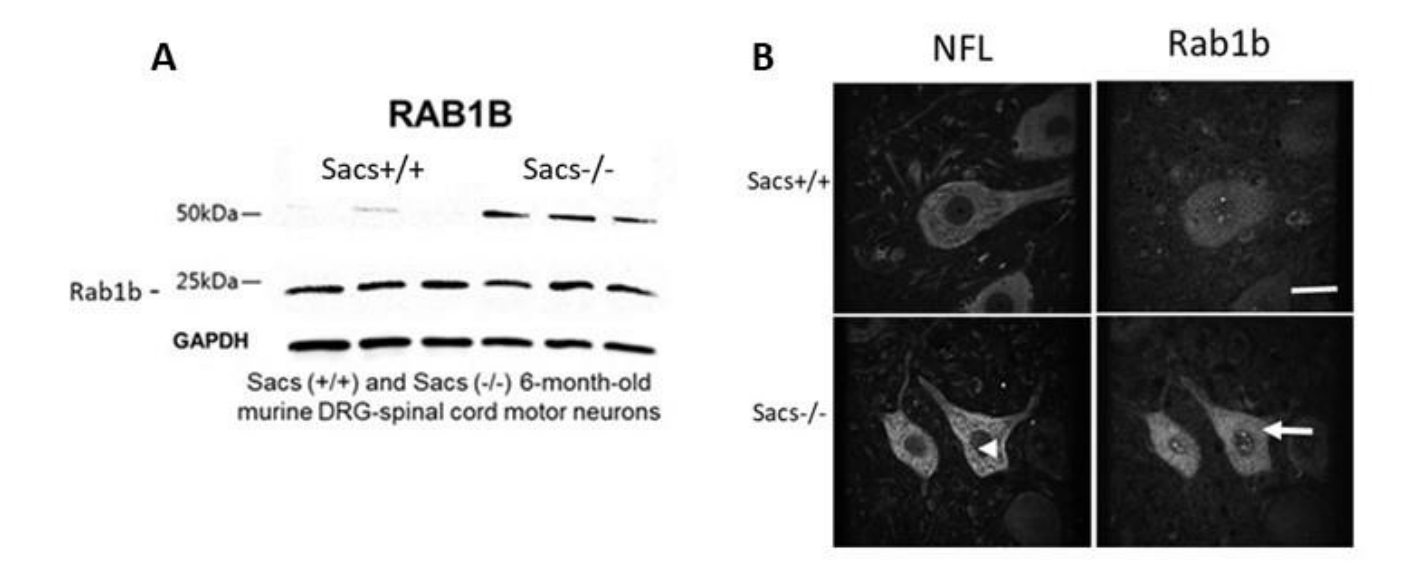
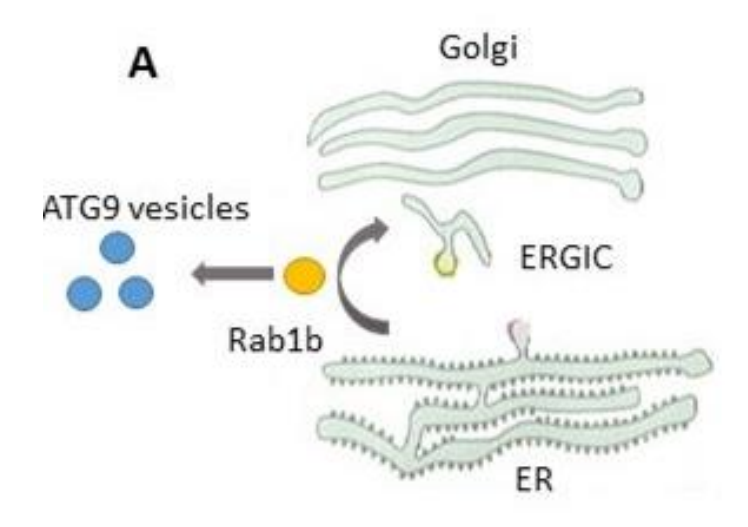


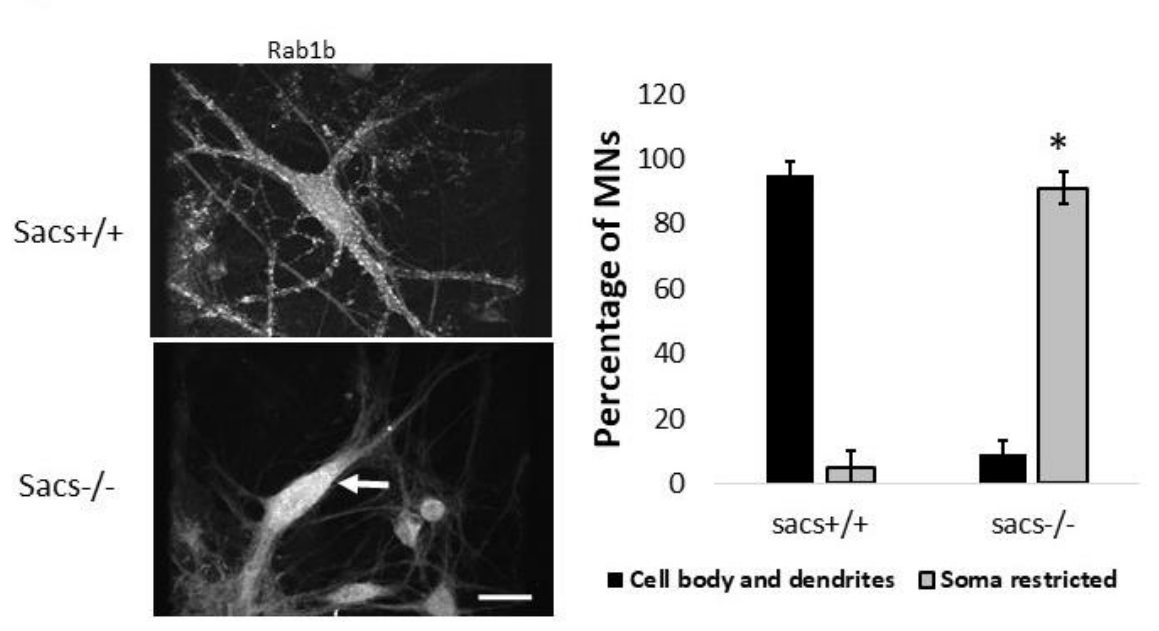
Figure 5. Identification of SacsJ interactome and functions showing the involvement of SacsJspecific binding proteins in functions associated with subcellular localization and transport. A) Red ponceau staining of a nitrocellulose membrane following SDS-PAGE and electrotransfer of spinal cord lysate (first lane), GST pulldown sample, and SacsJ pulldown sample. B) Venn diagram representing the distribution into specific binding proteins of SacsJ and control GST, as well as common partners, of proteins identified by mass spectrometry in the pull-down experiment using spinal cord as lysate. Numbers in diagram represent the number of different proteins identified by Mass spectrometry using the Scaffold software C) Volcano plot showing Fold Change of different proteins identified by mass spectrometry. Rab1b is highlighted in yellow and significantly enriched in the DNAJ sample. D) Table listing enriched proteins, from most enriched (top) to least enriched (bottom), identified by mass spectrometry. Rab1b is second most enriched protein. E) Interaction map of the SacsJ-specific partners using STRING software. Interacting proteins were grouped by known interaction networks. A cluster containing Rab1b with a PPI enrichment value of 0.00515 was identified (circle in green) F) Donut Pie-chart indicating major biological functions carried by SacsJinteracting proteins as defined by GO-terms. Major functions identified a role of SacsJ-specific binding partners are involved in organellar localization and transport.

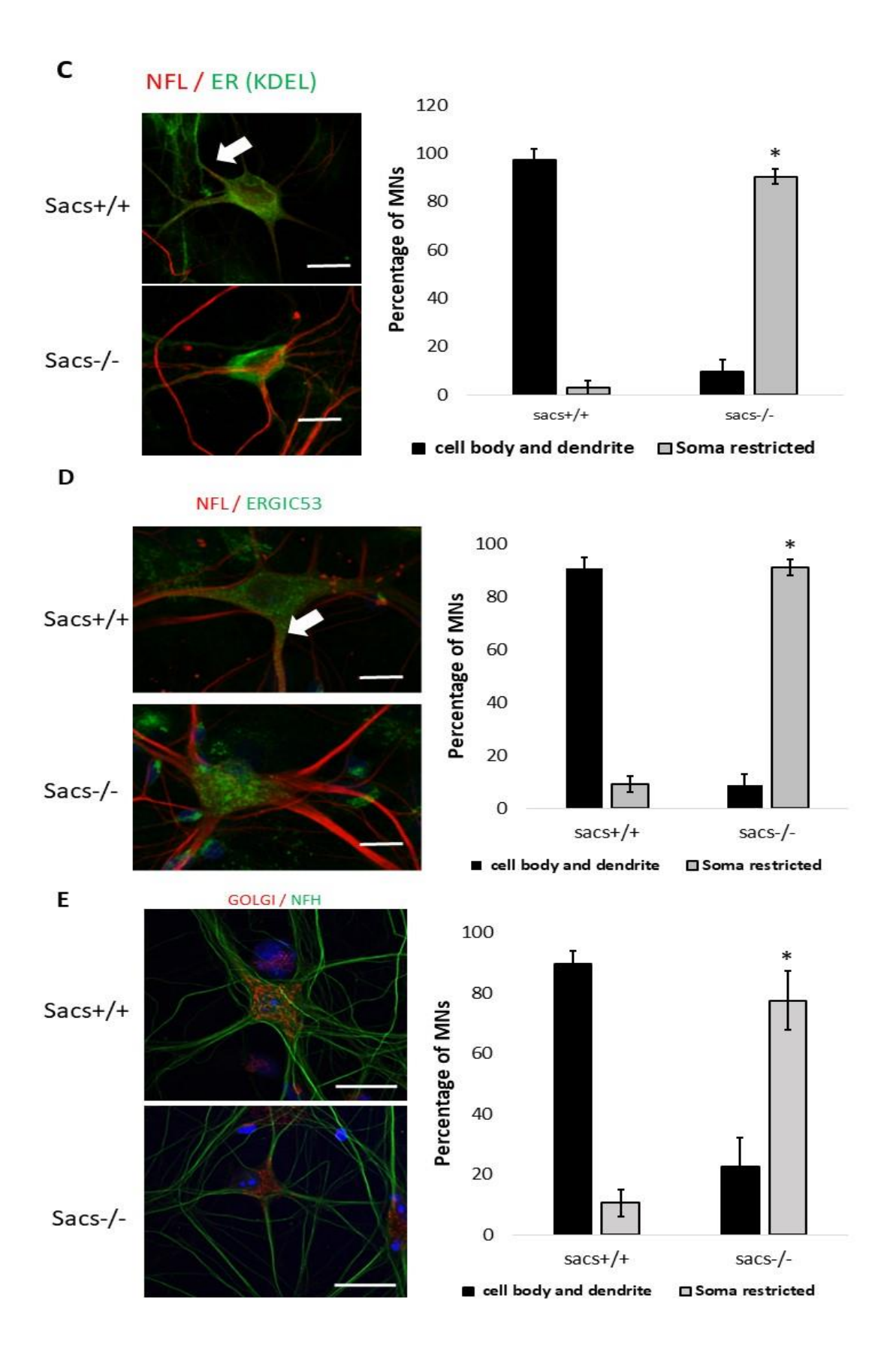


**Figure 6. Rab1b is upregulated with putative post-translation modifications and its distribution is restricted in** *Sacs* (-/-) **motor neurons. A)** Western blot analysis of Rab1b protein expression levels in *Sacs*+/+ and *Sacs*-/- 6-month-old DRG spinal cord motor neurons. Rab1b is upregulated and higher molecular weight bands, indicating post-translational modifications are observed in *Sacs*-/- motor neurons **B)** Representative Z-projection of confocal images of indirect double immunofluorescence labelling of Rab1b (rabbit anti-rab1b) and NFL (mouse anti-NFL) in motor neurons of 6-months old *Sacs*+/+ and *Sacs*-/- mice showing NFL bundles and increased fluorescence of Rab1b in *Sacs*-/- neuronal soma.









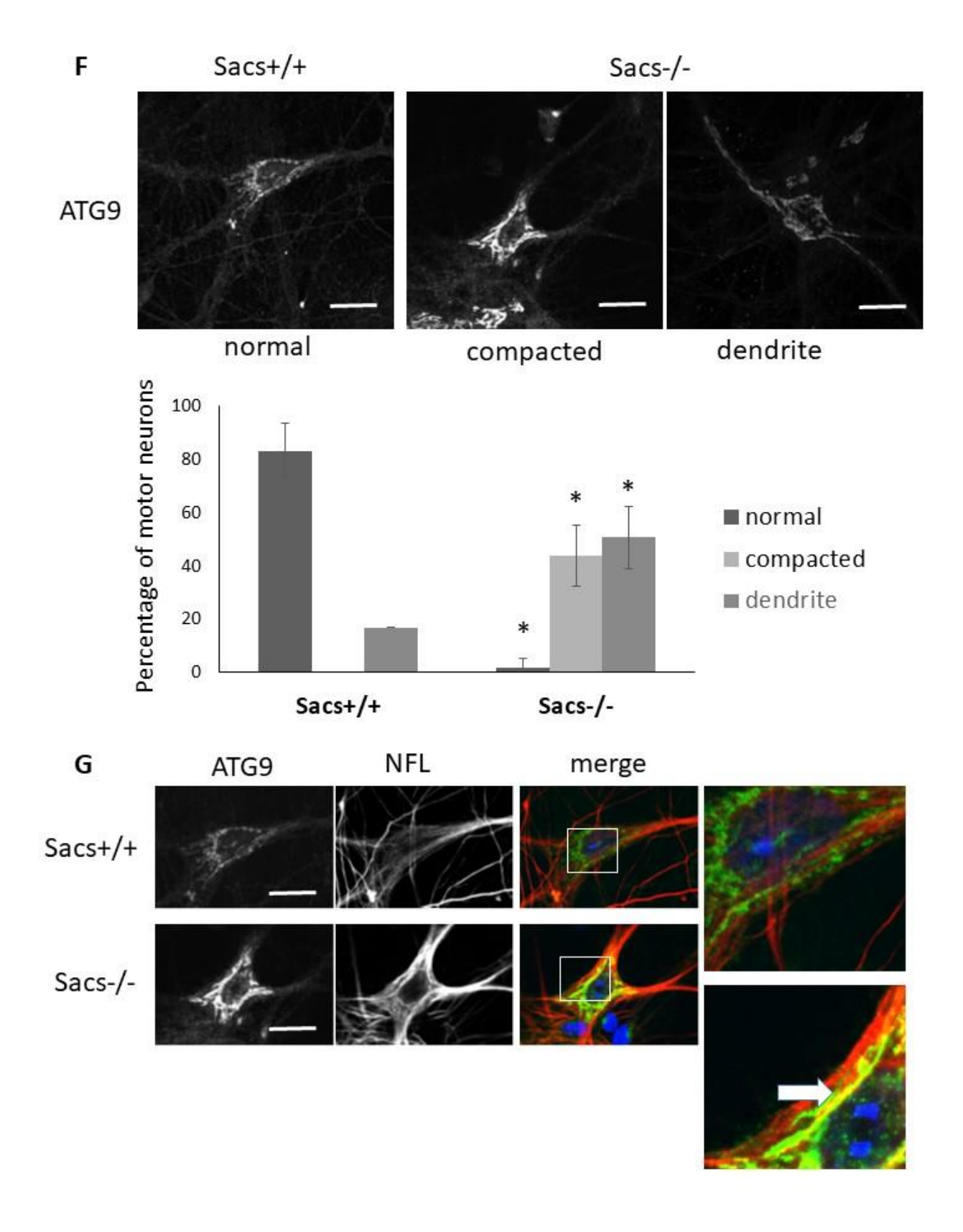


Figure 7. Rab1b, ER, ERGIC, Golgi, and ATG9 distribution is restricted in Sacs-/- motor neurons. A) Schematic representation of the role of Rab1b in the secretory pathway and autophagy. Rab1b plays a role in membrane fission, transport, and fusion at the ER, ERGIC, Golgi, and early steps of autophagy with ATG9. B) Representative Z-projection of confocal images of indirect immunofluorescence labelling of Rab1b (rabbit anti-rab1b) and NFL (mouse anti-NFL) in 6-week-old spinal cord Sacs+/+ and Sacs-/- motor neurons in culture showing accumulation of Rab1b in the soma of Sacs-/- motor neurons (bottom). Quantitation of the percentage of motor neurons showing cell body and dendritic or restricted to the soma distribution of Rab1b. \*p< 0.05 vs Sacs+/+ using a one-way ANOVA, HSD Tukey post hoc analysis Scale bar (20uM) (N=3) Scale bar (20uM). C-E) Representative Z-projection of confocal images following indirect double immunofluorescence labelling for ER, ERGIC, and Golgi with anti-KDEL, anti-ERGIC, anti-GM130 (mouse anti-KDEL, rabbit anti-ERGIC53, rabbit anti-GM130) and anti-NFL (rabbit anti-NFH, mouse anti-NFL) in Sacs+/+ and Sacs-/- 6-week-old spinal cord cultured motor neurons illustrating secretory pathway organelle distribution. Quantitation of ER, ERGIC, and Golgi phenotypes as either in the cell body and dendrites or as restricted to the soma. \*p< 0.05 vs Sacs+/+ using a one-way ANOVA, HSD Tukey post hoc analysis. F) Representative Z-projection of confocal images following indirect double immunofluorescence labelling for anti-ATG9 (rabbit anti-ATG9A) and anti-NFL (mouse anti-NFL) in Sacs+/+ and Sacs-/- 6-week-old spinal cord cultured motor neurons illustrating ATG9 vesicle distribution. Quantitation of ATG9 vesicle distribution phenotypes as normal, compacted, or dendritic. \*p< 0.05 vs Sacs+/+ using a one-way ANOVA, HSD Tukey post hoc analysis (N=3) Scale bar (20uM) G) ATG9 is juxtaposed to NFL bundles rather than colocalized. Representative Z-projection of confocal images following indirect double immunofluorescence labelling for anti-ATG9 (rabbit anti-ATG9A in green) and anti-NFL (mouse anti-NFL in red) in Sacs+/+ and Sacs-/- 6-week-old spinal cord cultured motor neurons to assess ATG9 and NFL network colocalization in cultured motor neurons. Thick white arrow points to juxtaposition of ATG9 vesicles with NF bundle. Scale bar (20µm).

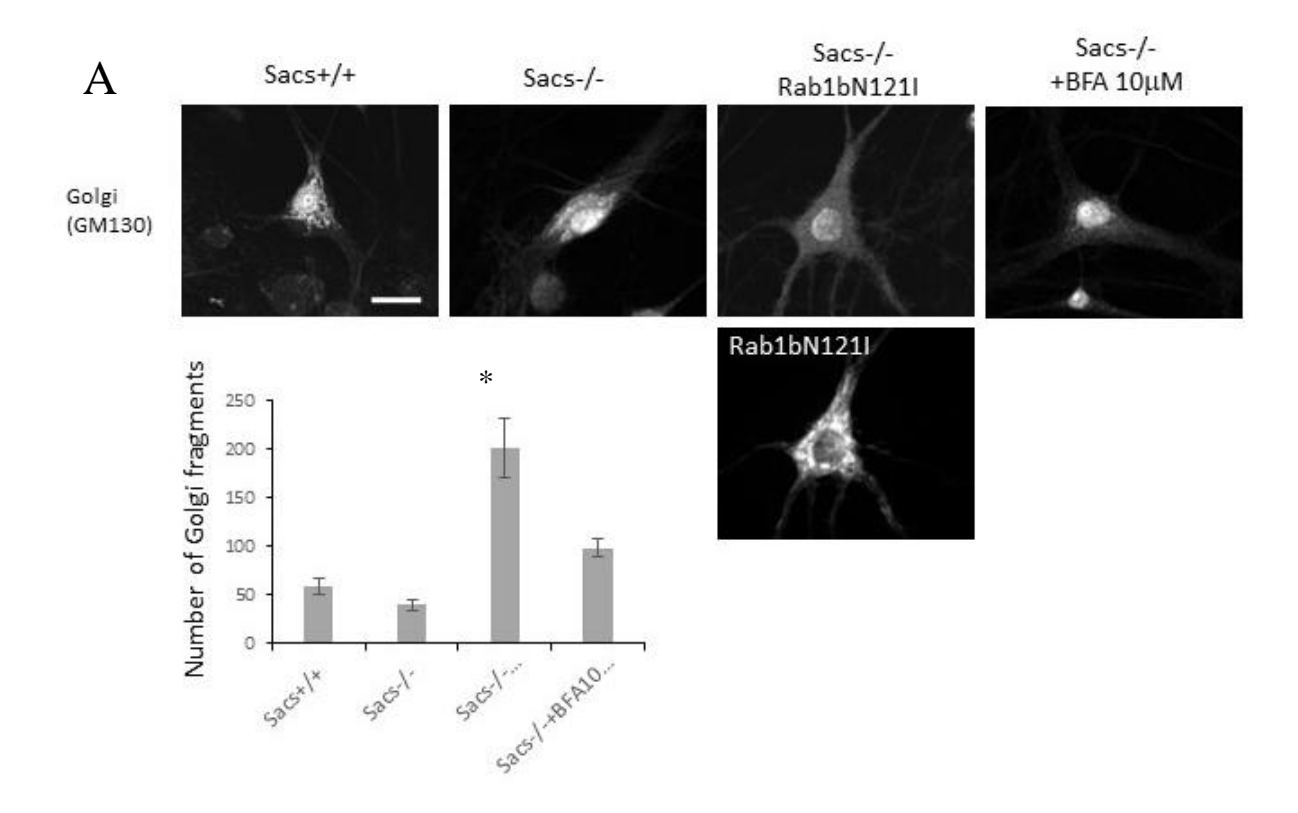
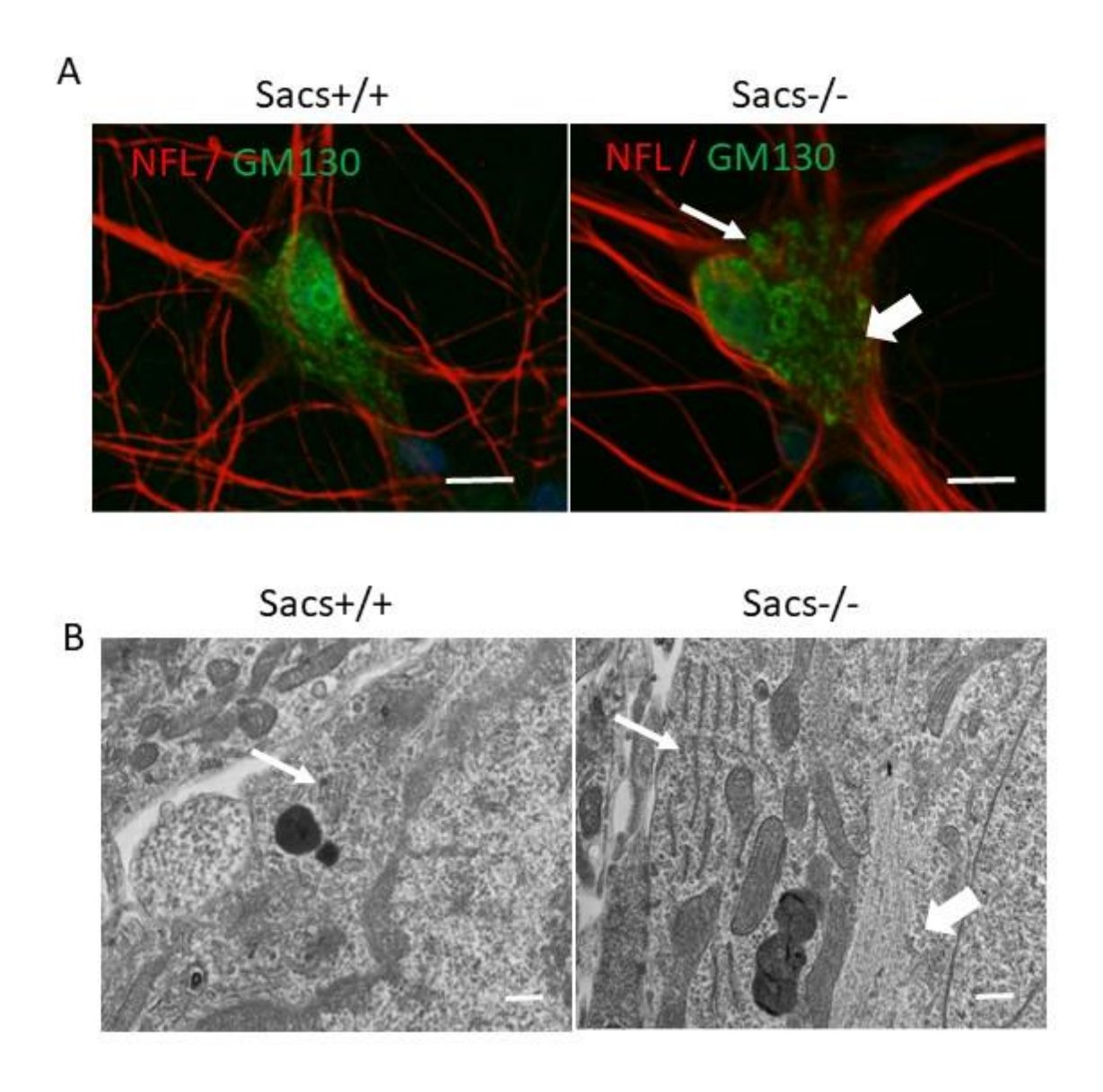
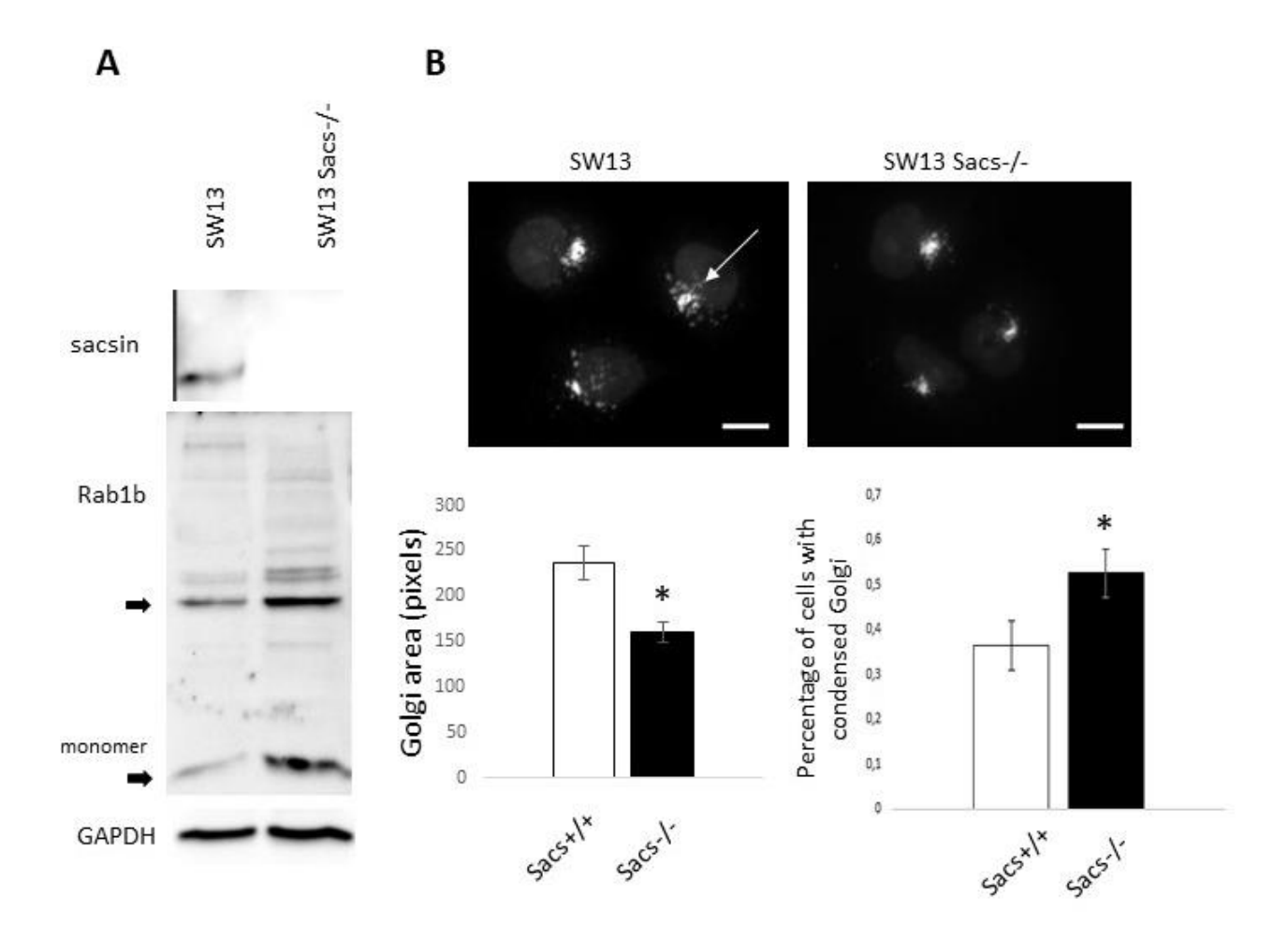


Figure 8. The Golgi apparatus is compacted in *Sacs-/-* motor neurons and requires dynamic Rab1b trafficking for healthy morphology. A) Representative Z-projection of confocal images following indirect double immunofluorescence labelling for anti-GM130 (rabbit anti-GM130) and anti-NFL (mouse anti-NFL) in *Sacs+/+* and *Sacs-/-* 6-week-old spinal cord cultured motor neurons to assess Golgi morphology following 24h microinjection of Rab1bN121 (dominant-negative mutant) and BFA 10uM treatment for 30 minutes. Quantitation of number of Golgi fragments is assessed. \*p< 0.05 vs *Sacs+/+* using a one-way ANOVA, HSD Tukey post hoc analysis (N=15). Scale bar (20μm)



**Figure 9. Electron microscopy imaging illustrating a neurofilament bundle in proximity of an eccentric Golgi apparatus in** *Sacs-/-* **motor neurons. A)** Representative Z-projection of confocal images following indirect immunofluorescence labelling for anti-GM130 (rabbit anti-GM130 in green) and anti-NFL (mouse anti-NFL in red) in *Sacs+/+* and *Sacs-/-* 6-week-old spinal cord cultured motor neurons illustrating Golgi distribution. The Golgi apparatus (Right panel, thin white arrow) appears to have a neurofilament bundle (thick white arrow) coursing through it in *Sacs-/-* motor neuron. Scale bar (20μM) **B)** Electron microscopy imaging in *Sacs+/+* and *Sacs-/-* motor neurons showing an eccentric Golgi apparatus (thin white arrow) and a neurofilament bundle coursing in proximity (Thick white arrow) in *Sacs* (-/-) motor neurons. Scale bar (20μm).



**Figure 10.** The Golgi apparatus is compacted in SW13- *Sacs-/-* cells lacking endogenous intermediate filaments. **A)** Western blot analysis show upregulated Rab1b and higher weight molecular bands in SW13- *Sacs-/-* cells. **B)** Representative Z-projection of confocal images following indirect immunofluorescence labelling for anti-GM130 (rabbit anti-GM130) and DAPI in SW13- *Sacs+/+* and SW13- *Sacs-/-* cultured cells to assess Golgi morphology. Quantitative assessment of Golgi area represented by the total number of pixels labeled for GM130 illustrates a compacted Golgi in majority of SW13- *Sacs-/-* cells. \*p< 0.05 vs Sacs+/+ using a one-way ANOVA, HSD Tukey post hoc analysis. Scale bar (20μm).

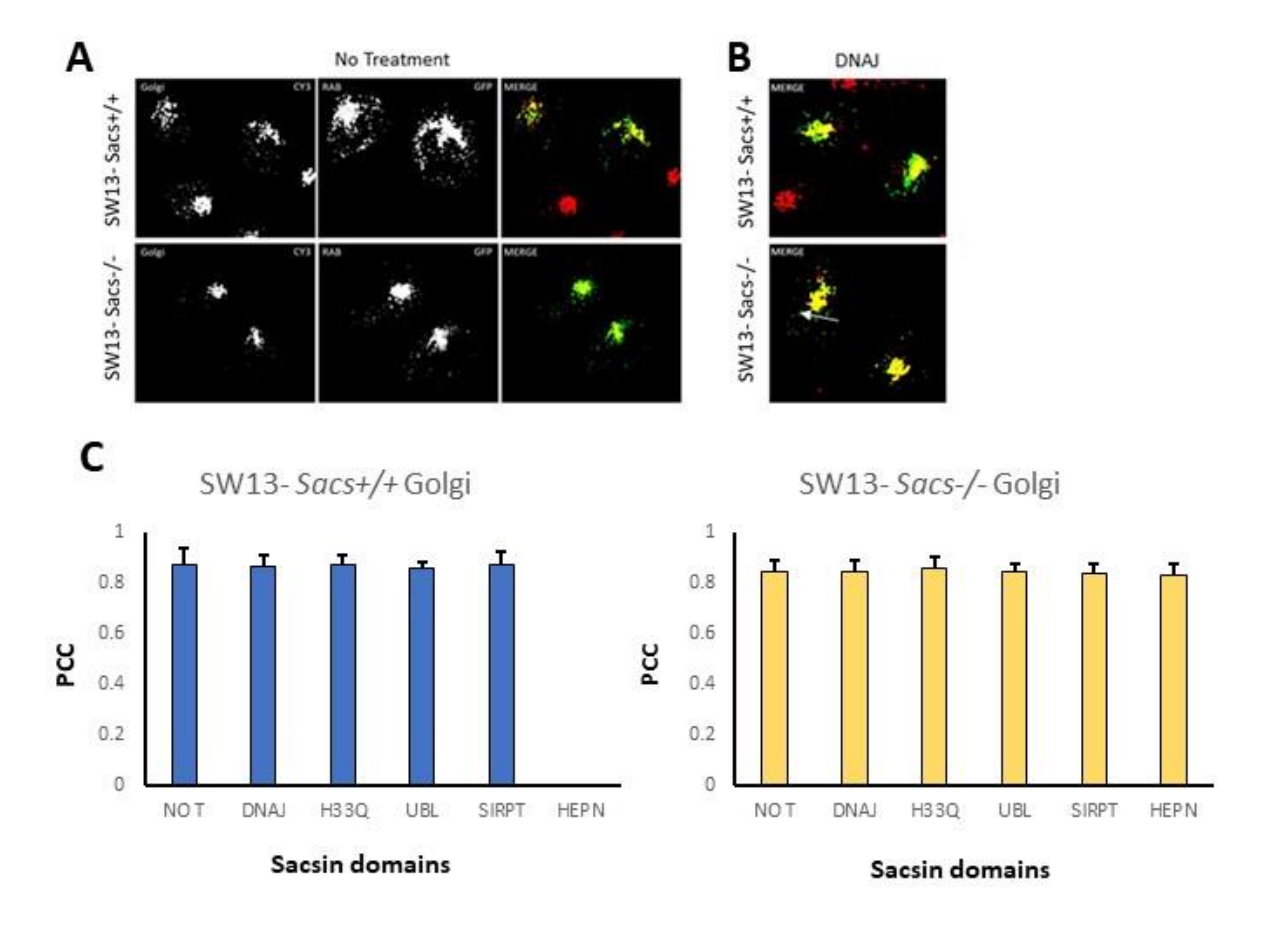


**Figure 11. Rab1b is strongly colocalized with the Golgi and sacsin domains do not significantly alter Rab1b association with the Golgi apparatus. A)** Representative Z-projection of confocal images following co-transfection of GFP-Rab1bwt and individual SACSIN domains and indirect immunofluorescence labelling for anti-GM130 (rabbit anti-GM130 in red) to assess colocalization of Rab1b and Golgi apparatus in SW13- Sacs+/+ and SW13- Sacs-/- cells. Yellow illustrates overlap of labelled structures in merge. **B)** Effect of *Dnaj (SacsJ)* on Rab1b colocalization with Golgi apparatus in SW13- Sacs+/+ and SW13- Sacs-/- cells. **C)** Quantitation of colocalization between Rab1b and the Golgi apparatus following transfection of SACSIN domains. A greater Pearson Correlation Coefficient (**PCC**) indicates greater colocalization of GFP-Rab1bwt with GM130. \*p< 0.05 vs No Treatment counterparts using a one-way ANOVA, HSD Tukey post hoc analysis. Scale bar (20μm). (N=25 per

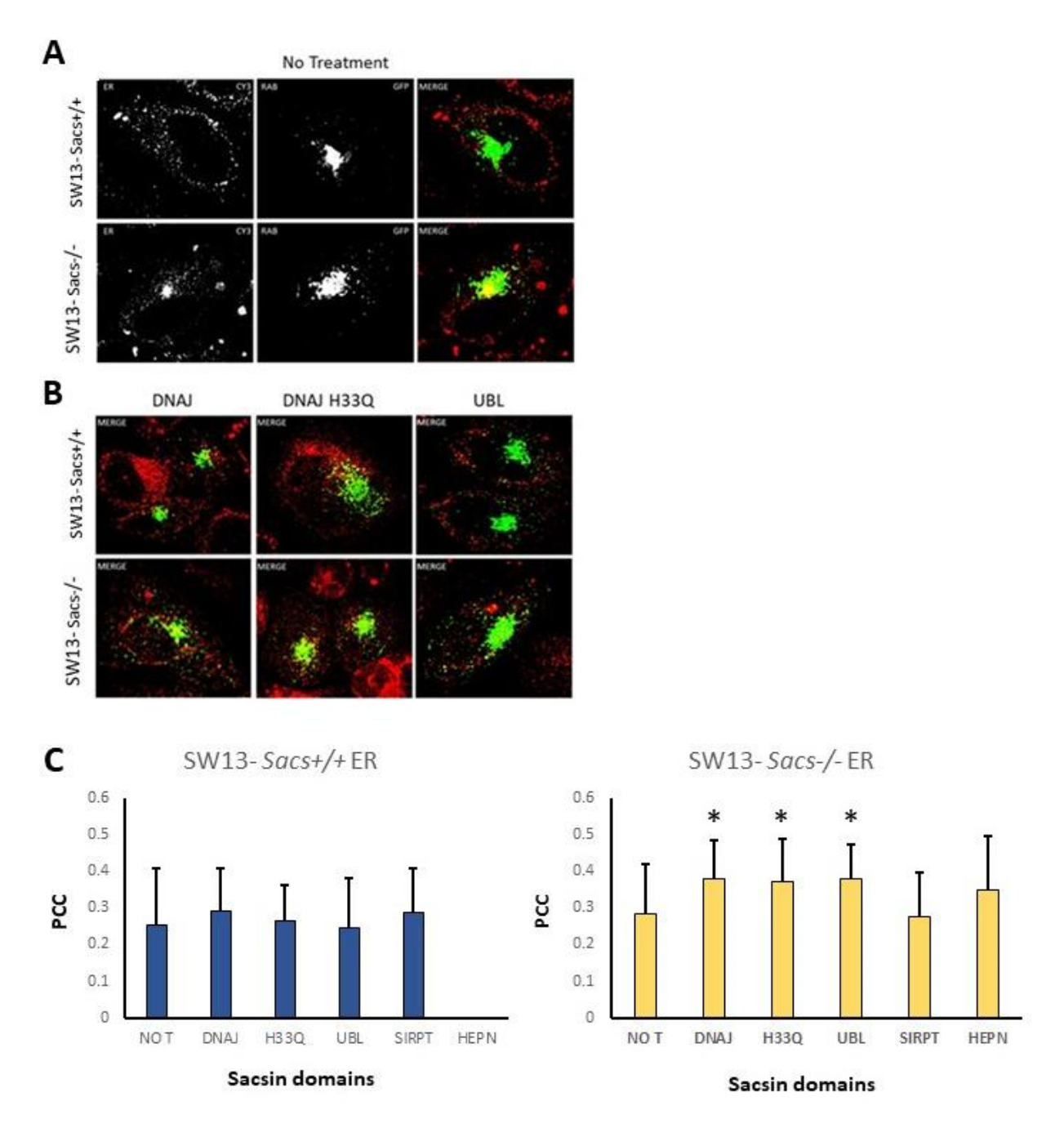


**Figure 12.** Rab1b is weakly colocalized with the ER and SACSIN domains DNAJ, DNAJ H33Q, *Ubl*, significantly increase Rab1b association with the ER in SW13-Sacs-/- cells. A) Representative Z-projection of confocal images following transfection of GFP-Rab1bwt and indirect immunofluorescence labelling for ER (mouse anti-KDEL in red) to assess colocalization of Rab1b and ER in SW13- Sacs+/+ and SW13- Sacs-/- cells. Yellow illustrates overlap of labelled structures in merge. B) Effect of *Dnaj*, *H33Q*, and *Ubl* on Rab1b association with ER in SW13- Sacs+/+ and SW13- Sacs-/- cells. C) Quantitation of colocalization between Rab1b and ER following transfection of SACSIN domains. A greater Pearson Correlation Coefficient (**PCC**) indicates greater colocalization of GFP-Rab1bwt with KDEL. \*p< 0.05 vs No Treatment counterparts using a one-way ANOVA, HSD Tukey post hoc analysis. Scale bar (20μm). (N=25 per condition).

## **Section 8: References**

- Kuchay, R. A., Mir, Y. R., Zeng, X., Hassan, A., Musarrat, J., Parwez, I., ... & Synofzik, M. (2019). ARSACS as a worldwide disease: novel SACS mutations identified in a consanguineous family from the remote tribal Jammu and Kashmir region in India. The Cerebellum, 18(4), 807-812.
- 2. Gentil BJ, Lai GT, Menade M, Lariviere R, Minotti S, Gehring K, et al. Sacsin, mutated in the ataxia ARSACS, regulates intermediate filament assembly and dynamics. FASEB J. 2019;33(2):2982-94. Epub 2018/10/18. doi: 10.1096/fj.201801556R. PubMed PMID: 30332300.
- 3. Vermeer, S., Meijer, R. P., Pijl, B. J., Timmermans, J., Cruysberg, J. R., Bos, M. M., ... & Kremer, B. (2008). ARSACS in the Dutch population: a frequent cause of early-onset cerebellar ataxia. Neurogenetics, 9(3), 207-214.
- 4. Pedroso, J. L., Braga-Neto, P., Abrahão, A., Rivero, R. L. M., Abdalla, C., Abdala, N., & Barsottini, O. G. P. (2011). Autosomal recessive spastic ataxia of Charlevoix-Saguenay (ARSACS): typical clinical and neuroimaging features in a Brazilian family. Arquivos de neuro-psiquiatria, 69, 288-291.
- 5. Bouchard, J. P., Barbeau, A., Bouchard, R., & Bouchard, R. W. (1978). Autosomal recessive spastic ataxia of Charlevoix-Saguenay. Canadian Journal of neurological sciences, 5(1), 61-69.
- 6. Vogel, A. P., Rommel, N., Oettinger, A., Stoll, L. H., Kraus, E. M., Gagnon, C., ... & Synofzik, M. (2018). Coordination and timing deficits in speech and swallowing in

- autosomal recessive spastic ataxia of Charlevoix–Saguenay (ARSACS). Journal of neurology, 265, 2060-2070.
- 7. Baets, J., Deconinck, T., Smets, K., Goossens, D., Van den Bergh, P., Dahan, K., ... & De Jonghe, P. (2010). Mutations in SACS cause atypical and late-onset forms of ARSACS. Neurology, 75(13), 1181-1188.
- 8. Engert J. C., Bérubé P., Mercier J., Doré C., Lepage P., Ge B., Bouchard J. P., Mathieu J., Melançon S. B., Schalling M., Lander E. S., Morgan K., Hudson T. J., Richter A. (2000) Nat. Genet. 24, 120–1251.
- 9. Vingolo EM, Di Fabio R, Salvatore S, Grieco G, Bertini E, Leuzzi V, et al. Myelinated retinal fibers in autosomal recessive spastic ataxia of Charlevoix-Saguenay. Eur J Neurol. 2011;18(9):1187-90. Epub 2011/03/18. doi: 10.1111/j.1468-1331.2010.03335.x. PubMed PMID: 21410841.
- Ogawa, T., Takiyama, Y., Sakoe, K., Mori, K., Namekawa, M., Shimazaki, H., ... & Nishizawa, M. (2004). Identification of a SACS gene missense mutation in ARSACS. Neurology, 62(1), 107-109.
- 11. Duquette, A., Brais, B., Bouchard, J. P., & Mathieu, J. (2013). Clinical presentation and early evolution of spastic ataxia of Charlevoix-Saguenay. Movement Disorders, 28(14), 2011-2014.
- Prodi, E., Grisoli, M., Panzeri, M., Minati, L., Fattori, F., Erbetta, A., ... & Mariotti, C. (2013). Supratentorial and pontine MRI abnormalities characterize recessive spastic ataxia of C harlevoix-S aguenay. A comprehensive study of an I talian series. European Journal of Neurology, 20(1), 138-146.

- Synofzik, M., Soehn, A. S., Gburek-Augustat, J., Schicks, J., Karle, K. N., Schüle, R., ...
   & Schöls, L. (2013). Autosomal recessive spastic ataxia of Charlevoix Saguenay (ARSACS): expanding the genetic, clinical and imaging spectrum. Orphanet journal of rare diseases, 8(1), 41.
- 14. Pilliod, J., Moutton, S., Lavie, J., Maurat, E., Hubert, C., Bellance, N., ... & Coupry, I. (2015). New practical definitions for the diagnosis of autosomal recessive spastic ataxia of C harlevoix–S aguenay. Annals of Neurology, 78(6), 871-886.
- Pablo, L. E., Garcia-Martin, E., Gazulla, J., Larrosa, J. M., Ferreras, A., Santorelli, F. M.,
   ... & Marin, M. A. (2011). Retinal nerve fiber hypertrophy in ataxia of Charlevoix-Saguenay patients. Molecular Vision, 17, 1871.
- Parkinson, M. H., Bartmann, A. P., Clayton, L. M., Nethisinghe, S., Pfundt, R., Chapple,
   J. P., ... & Giunti, P. (2018). Optical coherence tomography in autosomal recessive spastic ataxia of Charlevoix-Saguenay. Brain, 141(4), 989-999.
- 17. Dupré, N., Bouchard, J. P., Brais, B., & Rouleau, G. A. (2006). Hereditary ataxia, spastic paraparesis and neuropathy in the French-Canadian population. Canadian journal of neurological sciences, 33(2), 149-157.
- 18. Schatton, C., Synofzik, M., Fleszar, Z., Giese, M. A., Schöls, L., & Ilg, W. (2017). Individualized exergame training improves postural control in advanced degenerative spinocerebellar ataxia: A rater-blinded, intra-individually controlled trial. Parkinsonism & related disorders, 39, 80-84.
- 19. Lessard, I., Masterman, V., Côté, I., Gagnon, C., & Duchesne, E. (2022). A rehabilitation program to increase balance and mobility in ataxia of Charlevoix-Saguenay: An exploratory study. Plos one, 17(12), e0279406.

- 20. Kaji, R., Osako, Y., Suyama, K., Maeda, T., Uechi, Y., & Iwasaki, M. (2010). Botulinum toxin type A in post-stroke lower limb spasticity: a multicenter, double-blind, placebocontrolled trial. Journal of neurology, 257, 1330-1337.
- Picher-Martel, V., & Dupre, N. (2018). Current and promising therapies in autosomal recessive ataxias. CNS & Neurological Disorders-Drug Targets (Formerly Current Drug Targets-CNS & Neurological Disorders), 17(3), 161-171.
- 22. Francis, V., Alshafie, W., Kumar, R., Girard, M., Brais, B., & McPherson, P. S. (2022). The ARSACS disease protein sacsin controls lysosomal positioning and reformation by regulating microtubule dynamics. Journal of Biological Chemistry, 298(9).
- 23. Duncan, E. J., Larivière, R., Bradshaw, T. Y., Longo, F., Sgarioto, N., Hayes, M. J., ... & Chapple, J. P. (2017). Altered organization of the intermediate filament cytoskeleton and relocalization of proteostasis modulators in cells lacking the ataxia protein sacsin. Human molecular genetics, 26(16), 3130-3143.
- 24. Morani F, Doccini S, Sirica R, Paterno M, Pezzini F, Ricca I, et al. Functional Transcriptome Analysis in ARSACS KO Cell Model Reveals a Role of Sacsin in Autophagy. Sci Rep. 2019;9(1):11878. Epub 2019/08/17. doi: 10.1038/s41598-019-48047-x. PubMed PMID: 31417125; PubMed Central PMCID: PMCPMC6695435.
- 25. Girard M, Larivière R, Parfitt DA, Deane EC, Gaudet R, Nossova N, et al. Mitochondrial dysfunction and Purkinje cell loss in autosomal recessive spastic ataxia of Charlevoix-Saguenay (ARSACS). Proc Natl Acad Sci U S A. 2012;109(5):1661-6. doi: 10.1073/pnas.1113166109. PubMed PMID: 22307627; PubMed Central PMCID: PMCPMC3277168.

- Iwatsuki, H., & Suda, M. (2010). Seven kinds of intermediate filament networks in the cytoplasm of polarized cells: structure and function. Acta histochemica et cytochemica, 43(2), 19-31.
- 27. Lariviere R, Gaudet R, Gentil BJ, Girard M, Conte TC, Minotti S, et al. Sacs knockout mice present pathophysiological defects underlying autosomal recessive spastic ataxia of Charlevoix-Saguenay. Hum Mol Genet. 2015;24(3):727-39. doi: 10.1093/hmg/ddu491. PubMed PMID: 25260547; PubMed Central PMCID: PMCPMC4291249
- Ady, V., Toscano-Márquez, B., Nath, M., Chang, P. K., Hui, J., Cook, A., ... & Watt, A.
   J. (2018). Altered synaptic and firing properties of cerebellar Purkinje cells in a mouse model of ARSACS. The Journal of physiology, 596(17), 4253-4267.
- 29. Romano A, Tessa A, Barca A, Fattori F, de Leva MF, Terracciano A, et al. Comparative analysis and functional mapping of SACS mutations reveal novel insights into sacsin repeated architecture. Hum Mutat. 2013;34(3):525-37. doi: 10.1002/humu.22269. PubMed PMID: 23280630; PubMed Central PMCID: PMCPMC3629688.
- 30. Bagaria, J., Bagyinszky, E., & An, S. S. A. (2022). Genetics of Autosomal Recessive Spastic Ataxia of Charlevoix-Saguenay (ARSACS) and Role of Sacsin in Neurodegeneration. International journal of molecular sciences, 23(1), 552.
- 31. Parfitt DA, Michael GJ, Vermeulen EG, Prodromou NV, Webb TR, Gallo JM, et al. The ataxia protein sacsin is a functional co-chaperone that protects against polyglutamine-expanded ataxin-1. Hum Mol Genet. 2009;18(9):1556-65. doi: 10.1093/hmg/ddp067. PubMed PMID: 19208651; PubMed Central PMCID: PMCPMC2667285.

- 32. Anderson JF, Siller E, Barral JM. The sacsin repeating region (SRR): a novel Hsp90-related supradomain associated with neurodegeneration. J Mol Biol. 2010;400(4):665-74. Epub 2010/05/22. doi: 10.1016/j.jmb.2010.05.023. PubMed PMID: 20488193.
- 33. LaSalle, J. M., Reiter, L. T., & Chamberlain, S. J. (2015). Epigenetic regulation of UBE3A and roles in human neurodevelopmental disorders. Epigenomics, 7(7), 1213-1228.
- 34. Grynberg, M., Erlandsen, H., & Godzik, A. (2003). HEPN: a common domain in bacterial drug resistance and human neurodegenerative proteins. Trends in biochemical sciences, 28(5), 224-226.
- 35. Szeverenyi, I., Cassidy, A. J., Chung, C. W., Lee, B. T., Common, J. E., Ogg, S. C., ... & Lane, E. B. (2008). The Human Intermediate Filament Database: comprehensive information on a gene family involved in many human diseases. Human mutation, 29(3), 351-360.
- 36. Kidd, M. E., Shumaker, D. K., & Ridge, K. M. (2014). The role of vimentin intermediate filaments in the progression of lung cancer. American journal of respiratory cell and molecular biology, 50(1), 1-6.
- 37. Ridge, K. M., Eriksson, J. E., Pekny, M., & Goldman, R. D. (2022). Roles of vimentin in health and disease. Genes & Development, 36(7-8), 391-407.
- 38. Yuan, A., Rao, M. V., & Nixon, R. A. (2012). Neurofilaments at a glance. Journal of cell science, 125(14), 3257-3263.
- 39. Herrmann, H., & Aebi, U. (2016). Intermediate filaments: structure and assembly. Cold Spring Harbor Perspectives in Biology, 8(11), a018242.

- 40. Portet, S., Mücke, N., Kirmse, R., Langowski, J., Beil, M., & Herrmann, H. (2009).
  Vimentin intermediate filament formation: in vitro measurement and mathematical modeling of the filament length distribution during assembly. Langmuir, 25(15), 8817-8823.
- 41. Laser-Azogui, A., Kornreich, M., Malka-Gibor, E., & Beck, R. (2015). Neurofilament assembly and function during neuronal development. Current opinion in cell biology, 32, 92-101.
- 42. Biskou, O., Casanova, V., Hooper, K. M., Kemp, S., Wright, G. P., Satsangi, J., ... & Stevens, C. (2019). The type III intermediate filament vimentin regulates organelle distribution and modulates autophagy. PLoS One, 14(1), e0209665.
- 43. Sanghvi-Shah, R., & Weber, G. F. (2017). Intermediate filaments at the junction of mechanotransduction, migration, and development. Frontiers in cell and developmental biology, 5, 81.
- 44. Wiche, G., Osmanagic-Myers, S., & Castañón, M. J. (2015). Networking and anchoring through plectin: a key to IF functionality and mechanotransduction. Current opinion in cell biology, 32, 21-29.
- 45. Pan, X., Hobbs, R. P., & Coulombe, P. A. (2013). The expanding significance of keratin intermediate filaments in normal and diseased epithelia. Current opinion in cell biology, 25(1), 47-56.
- 46. Rogel, M. R., Jaitovich, A., & Ridge, K. M. (2010). The role of the ubiquitin proteasome pathway in keratin intermediate filament protein degradation. Proceedings of the american thoracic society, 7(1), 71-76.

- 47. Omary, M. B., Coulombe, P. A., & McLean, W. I. (2004). Intermediate filament proteins and their associated diseases. New England Journal of Medicine, 351(20), 2087-2100.
- 48. Anton-Lamprecht, I. (1983). Genetically induced abnormalities of epidermal differentiation and ultrastructure in ichthyoses and epidermolyses: pathogenesis, heterogeneity, fetal manifestation, and prenatal diagnosis. Journal of Investigative Dermatology, 81(1), S149-S156.
- 49. Sabatelli, M., Bertini, E., Ricci, E., Salviati, G., Magi, S., Papacci, M., & Tonali, P. (1992). Peripheral neuropathy with giant axons and cardiomyopathy associated with desmin type intermediate filaments in skeletal muscle. Journal of the neurological sciences, 109(1), 1-10.
- 50. Quinlan, R. A., Brenner, M., Goldman, J. E., & Messing, A. (2007). GFAP and its role in Alexander disease. Experimental cell research, 313(10), 2077-2087.
- Murtinheira, F., Migueis, M., Letra-Vilela, R., Diallo, M., Quezada, A., Valente, C. A.,
   ... & Herrera, F. (2022). Sacsin deletion induces aggregation of glial intermediate filaments. Cells, 11(2), 299.
- 52. Dustin, P. (2012). Microtubules. Springer Science & Business Media.
- 53. Vale, R. D. (2003). The molecular motor toolbox for intracellular transport. Cell, 112(4), 467-480.
- 54. Gudimchuk, N. B., & McIntosh, J. R. (2021). Regulation of microtubule dynamics, mechanics and function through the growing tip. Nature reviews Molecular cell biology, 22(12), 777-795.

- 55. Woods, L. C., Berbusse, G. W., & Naylor, K. (2016). Microtubules are essential for mitochondrial dynamics–fission, fusion, and motility–in dictyostelium discoideum. Frontiers in cell and developmental biology, 4, 19.
- 56. Bradshaw, T. Y., Romano, L. E., Duncan, E. J., Nethisinghe, S., Abeti, R., Michael, G. J., ... & Chapple, J. P. (2016). A reduction in Drp1-mediated fission compromises mitochondrial health in autosomal recessive spastic ataxia of Charlevoix Saguenay. Human molecular genetics, 25(15), 3232-3244.
- 57. Márquez, B. T., Leung, T. C. S., Hui, J., Charron, F., McKinney, R. A., & Watt, A. J. (2023). A mitochondrial-targeted antioxidant (MitoQ) improves motor coordination and reduces Purkinje cell death in a mouse model of ARSACS. Neurobiology of Disease, 183, 106157.
- 58. Martínez-Menárguez, J. Á., Martínez-Alonso, E., Cara-Esteban, M., & Tomás, M. (2021). Focus on the Small GTPase Rab1: A Key Player in the Pathogenesis of Parkinson's Disease. International Journal of Molecular Sciences, 22(21), 12087.
- 59. Plutner, H., Cox, A. D., Pind, S., Khosravi-Far, R., Bourne, J. R., Schwaninger, R., ... & Balch, W. E. (1991). Rab1b regulates vesicular transport between the endoplasmic reticulum and successive Golgi compartments. The Journal of cell biology, 115(1), 31-43.
- 60. Saraste, J., Lahtinen, U., & Goud, B. (1995). Localization of the small GTP-binding protein rab1p to early compartments of the secretory pathway. Journal of cell science, 108(4), 1541-1552.

- 61. Wang, C., Yoo, Y., Fan, H., Kim, E., Guan, K. L., & Guan, J. L. (2010). Regulation of Integrin β1 recycling to lipid rafts by Rab1a to promote cell migration. Journal of Biological Chemistry, 285(38), 29398-29405.
- 62. Zoppino FC, Militello RD, Slavin I, Alvarez C, Colombo MI. Autophagosome formation depends on the small GTPase Rab1 and functional ER exit sites. Traffic. 2010;11(9):1246–61.
- 63. Barlowe, C. K., & Miller, E. A. (2013). Secretory protein biogenesis and traffic in the early secretory pathway. Genetics, 193(2), 383-410.
- 64. Appenzeller-Herzog, C., & Hauri, H. P. (2006). The ER-Golgi intermediate compartment (ERGIC): in search of its identity and function. Journal of cell science, 119(11), 2173-2183.
- 65. Huang, S., & Wang, Y. (2017). Golgi structure formation, function, and post-translational modifications in mammalian cells. F1000Research, 6.
- 66. Kiral, F. R., Kohrs, F. E., Jin, E. J., & Hiesinger, P. R. (2018). Rab GTPases and membrane trafficking in neurodegeneration. Current Biology, 28(8), R471-R486.
- 67. Stenmark, H., & Olkkonen, V. M. (2001). The rab gtpase family. Genome biology, 2(5), 1-7.
- 68. Dirac-Svejstrup, A. B., Sumizawa, T., & Pfeffer, S. R. (1997). Identification of a GDI displacement factor that releases endosomal Rab GTPases from Rab–GDI. The EMBO journal, 16(3), 465-472.
- 69. Pereira-Leal, J. B., Hume, A. N., & Seabra, M. C. (2001). Prenylation of Rab GTPases: molecular mechanisms and involvement in genetic disease. FEBS letters, 498(2-3), 197-200.

- Calero, M., Chen, C. Z., Zhu, W., Winand, N., Havas, K. A., Gilbert, P. M., ... & Collins,
   R. N. (2003). Dual prenylation is required for Rab protein localization and function.
   Molecular biology of the cell, 14(5), 1852-1867.
- 71. Shinde, S. R., & Maddika, S. (2018). Post translational modifications of Rab GTPases. Small GTPases, 9(1-2), 49-56.
- 72. Kagan, J. C., Stein, M. P., Pypaert, M., & Roy, C. R. (2004). Legionella subvert the functions of Rab1 and Sec22b to create a replicative organelle. The Journal of experimental medicine, 199(9), 1201-1211.
- 73. Müller, M. P., Peters, H., Blümer, J., Blankenfeldt, W., Goody, R. S., & Itzen, A. (2010). The Legionella effector protein DrrA AMPylates the membrane traffic regulator Rab1b. Science, 329(5994), 946-949.
- 74. Lai, Y. C., Kondapalli, C., Lehneck, R., Procter, J. B., Dill, B. D., Woodroof, H. I., ... & Muqit, M. M. (2015). Phosphoproteomic screening identifies Rab GTP ases as novel downstream targets of PINK 1. The EMBO journal, 34(22), 2840-2861.
- 75. Bailly, E., McCaffrey, M., Touchot, N., Zahraoui, A., Goud, B., & Bornens, M. (1991). Phosphorylation of two small GTP-binding proteins of the Rab family by p34 cdc2. Nature, 350(6320), 715-718.
- 76. Levin, R. S., Hertz, N. T., Burlingame, A. L., Shokat, K. M., & Mukherjee, S. (2016). Innate immunity kinase TAK1 phosphorylates Rab1 on a hotspot for posttranslational modifications by host and pathogen. Proceedings of the National Academy of Sciences, 113(33), E4776-E4783.
- 77. Stenmark, H. (2009). Rab GTPases as coordinators of vesicle traffic. Nature reviews Molecular cell biology, 10(8), 513-525.

- 78. Shin, D., Na, W., Lee, J. H., Kim, G., Baek, J., Park, S. H., ... & Lee, S. (2017). Site-specific monoubiquitination downregulates Rab5 by disrupting effector binding and guanine nucleotide conversion. Elife, 6, e29154.
- Sapmaz, A., Berlin, I., Bos, E., Wijdeven, R. H., Janssen, H., Konietzny, R., ... & Ovaa,
   H. (2019). USP32 regulates late endosomal transport and recycling through deubiquitylation of Rab7. Nature communications, 10(1), 1454.
- 80. Song, P., Trajkovic, K., Tsunemi, T., & Krainc, D. (2016). Parkin modulates endosomal organization and function of the endo-lysosomal pathway. Journal of Neuroscience, 36(8), 2425-2437.
- 81. Martinez, Martinez, O., & Goud, B. (1998). Rab proteins. Biochimica et Biophysica Acta (BBA)-Molecular Cell Research, 1404(1-2), 101-112.
- 82. Kakuta, S., Yamaguchi, J., Suzuki, C., Sasaki, M., Kazuno, S., & Uchiyama, Y. (2017). Small GTPase Rab1B is associated with ATG9A vesicles and regulates autophagosome formation. The FASEB Journal, 31(9), 3757-3773.
- 83. García, I. A., Martinez, H. E., & Alvarez, C. (2011). Rab1b regulates COPI and COPII dynamics in mammalian cells. Cellular logistics, 1(4), 159-163.
- 84. Nichols, B. J., & Pelham, H. R. (1998). SNAREs and membrane fusion in the Golgi apparatus. Biochimica et Biophysica Acta (BBA)-Molecular Cell Research, 1404(1-2), 9-31.
- 85. Kakuta, S., Yamamoto, H., Negishi, L., Kondo-Kakuta, C., Hayashi, N., & Ohsumi, Y. (2012). Atg9 vesicles recruit vesicle-tethering proteins Trs85 and Ypt1 to the autophagosome formation site. Journal of Biological Chemistry, 287(53), 44261-44269.

- 86. Alvarez, C., Garcia-Mata, R., Brandon, E., & Sztul, E. (2003). COPI recruitment is modulated by a Rab1b-dependent mechanism. Molecular biology of the cell, 14(5), 2116-2127.
- 87. Monetta, P., Slavin, I., Romero, N., & Alvarez, C. (2007). Rab1b interacts with GBF1 and modulates both ARF1 dynamics and COPI association. Molecular biology of the cell, 18(7), 2400-2410.
- 88. Moyer, B. D., Allan, B. B., & Balch, W. E. (2001). Rab1 interaction with a GM130 effector complex regulates COPII vesicle cis-Golgi tethering. Traffic, 2(4), 268-276.
- 89. Allan, B. B., Moyer, B. D., & Balch, W. E. (2000). Rab1 recruitment of p115 into a cis-SNARE complex: programming budding COPII vesicles for fusion. Science, 289(5478), 444-448.
- 90. Rosing, M., Ossendorf, E., Rak, A., & Barnekow, A. (2007). Giantin interacts with both the small GTPase Rab6 and Rab1. Experimental cell research, 313(11), 2318-2325.
- 91. Søgaard, M., Tani, K., Ye, R. R., Geromanos, S., Tempst, P., Kirchhausen, T., ... & Söllner, T. (1994). A rab protein is required for the assembly of SNARE complexes in the docking of transport vesicles. Cell, 78(6), 937-948.
- 92. Alvarez, C., Fujita, H., Hubbard, A., & Sztul, E. (1999). ER to Golgi transport: requirement for p115 at a pre-Golgi VTC stage. The Journal of cell biology, 147(6), 1205-1222.
- 93. Romero, N., Dumur, C. I., Martinez, H., García, I. A., Monetta, P., Slavin, I., ... & Alvarez, C. (2013). Rab1b overexpression modifies Golgi size and gene expression in HeLa cells and modulates the thyrotrophin response in thyroid cells in culture. Molecular biology of the cell, 24(5), 617-632.

- 94. Feng, Y., & Klionsky, D. J. (2017). Autophagic membrane delivery through ATG9. Cell research, 27(2), 161-162.
- 95. Szatmári, Z., & Sass, M. (2014). The autophagic roles of Rab small GTPases and their upstream regulators: a review. Autophagy, 10(7), 1154-1166.
- 96. Tan, D., Cai, Y., Wang, J., Zhang, J., Menon, S., Chou, H. T., ... & Walz, T. (2013). The EM structure of the TRAPPIII complex leads to the identification of a requirement for COPII vesicles on the macroautophagy pathway. Proceedings of the National Academy of Sciences, 110(48), 19432-19437.
- 97. Lynch-Day, M. A., Bhandari, D., Menon, S., Huang, J., Cai, H., Bartholomew, C. R., ... & Klionsky, D. J. (2010). Trs85 directs a Ypt1 GEF, TRAPPIII, to the phagophore to promote autophagy. Proceedings of the National Academy of Sciences, 107(17), 7811-7816.
- 98. Lamb, C. A., Yoshimori, T., & Tooze, S. A. (2013). The autophagosome: origins unknown, biogenesis complex. Nature reviews Molecular cell biology, 14(12), 759-774.
- 99. Ge, L., Baskaran, S., Schekman, R., & Hurley, J. H. (2014). The protein-vesicle network of autophagy. Current opinion in cell biology, 29, 18-24.
- 100. Valente, E. M., Abou-Sleiman, P. M., Caputo, V., Muqit, M. M., Harvey, K., Gispert, S.,... & Wood, N. W. (2004). Hereditary early-onset Parkinson's disease caused by mutations in PINK1. Science, 304(5674), 1158-1160.
- 101. Fecto, F., Yan, J., Vemula, S. P., Liu, E., Yang, Y., Chen, W., ... & Siddique, T. (2011).
  SQSTM1 mutations in familial and sporadic amyotrophic lateral sclerosis. Archives of neurology, 68(11), 1440-1446.

- 102. Yang, X. Z., Li, X. X., Zhang, Y. J., Rodriguez-Rodriguez, L., Xiang, M. Q., Wang, H. Y., & Zheng, X. S. (2016). Rab1 in cell signaling, cancer and other diseases. Oncogene, 35(44), 5699-5704.
- 103. Gitler, A. D., Bevis, B. J., Shorter, J., Strathearn, K. E., Hamamichi, S., Su, L. J., ... & Lindquist, S. (2008). The Parkinson's disease protein α-synuclein disrupts cellular Rab homeostasis. Proceedings of the National Academy of Sciences, 105(1), 145-150.
- 104. Mazzulli, J. R., Zunke, F., Tsunemi, T., Toker, N. J., Jeon, S., Burbulla, L. F., ... & Krainc,
   D. (2016). Activation of β-glucocerebrosidase reduces pathological α-synuclein and restores lysosomal function in Parkinson's patient midbrain neurons. Journal of Neuroscience, 36(29), 7693-7706.
- 105. Webster, C. P., Smith, E. F., Bauer, C. S., Moller, A., Hautbergue, G. M., Ferraiuolo, L.,
  ... & De Vos, K. J. (2016). The C9orf72 protein interacts with Rab1a and the ULK 1
  complex to regulate initiation of autophagy. The EMBO journal, 35(15), 1656-1676.
- 106. Soo, K. Y., Halloran, M., Sundaramoorthy, V., Parakh, S., Toth, R. P., Southam, K. A., ... & Atkin, J. D. (2015). Rab1-dependent ER–Golgi transport dysfunction is a common pathogenic mechanism in SOD1, TDP-43 and FUS-associated ALS. Acta neuropathologica, 130(5), 679-697.
- 107. Dabbaghizadeh, A., Paré, A., Cheng-Boivin, Z., Dagher, R., Minotti, S., Dicaire, M. J., ... & Gentil, B. J. (2022). The J domain of sacsin disrupts intermediate filament assembly. International Journal of Molecular Sciences, 23(24), 15742.
- 108. Cyr, D. M., & Ramos, C. H. (2022). Specification of Hsp70 Function by Hsp40 Cochaperones. The Networking of Chaperones by Co-Chaperones, 127-139.

- 109. Hedberg, K. K., & Chen, L. B. (1986). Absence of intermediate filaments in a human adrenal cortex carcinoma-derived cell line. Experimental cell research, 163(2), 509-517.
- 110. Roy, J., Minotti, S., Dong, L., Figlewicz, D. A., & Durham, H. D. (1998). Glutamate potentiates the toxicity of mutant Cu/Zn-superoxide dismutase in motor neurons by postsynaptic calcium-dependent mechanisms. Journal of Neuroscience, 18(23), 9673-9684.
- 111. Herrmann, H., & Aebi, U. (2004). Intermediate filaments: molecular structure, assembly mechanism, and integration into functionally distinct intracellular Scaffolds. Annual review of biochemistry, 73(1), 749-789.
- 112. Patel, S. G., Sayers, E. J., He, L., Narayan, R., Williams, T. L., Mills, E. M., ... & Tsai, Y. H. (2019). Cell-penetrating peptide sequence and modification dependent uptake and subcellular distribution of green florescent protein in different cell lines. Scientific reports, 9(1), 6298.
- 113. McDonald, J. H., & Dunn, K. W. (2013). Statistical tests for measures of colocalization in biological microscopy. Journal of microscopy, 252(3), 295-302.
- 114. Izawa, I., Nishizawa, M., Ohtakara, K., Ohtsuka, K., Inada, H., & Inagaki, M. (2000). Identification of Mrj, a DnaJ/Hsp40 family protein, as a keratin 8/18 filament regulatory protein. Journal of Biological Chemistry, 275(44), 34521-34527.
- 115. Dubois, M., Strazielle, C., Julien, J. P., & Lalonde, R. (2005). Mice with the deleted neurofilament of low molecular weight (Nefl) gene: 2. Effects on motor functions and spatial orientation. Journal of neuroscience research, 80(6), 751-758.

- 116. Yang, Y., Chen, J., Guo, Z., Deng, S., Du, X., Zhu, S., ... & Liu, J. J. (2018). Endophilin A1 promotes actin polymerization in dendritic spines required for synaptic potentiation. Frontiers in molecular neuroscience, 11, 177.
- 117. Metzler, M., Legendre-Guillemin, V., Gan, L., Chopra, V., Kwok, A., McPherson, P. S.,
  & Hayden, M. R. (2001). HIP1 functions in clathrin-mediated endocytosis through
  binding to clathrin and adaptor protein 2. Journal of Biological Chemistry, 276(42),
  39271-39276.
- 118. Peng, L., Yang, Q., Xu, X., Du, Y., Wu, Y., Shi, X., ... & Luo, J. (2017). Huntingtin-interacting protein 1-related protein plays a critical role in dendritic development and excitatory synapse formation in hippocampal neurons. Frontiers in Molecular Neuroscience, 10, 186.
- 119. Chen, E., & Joseph, S. (2015). Fragile X mental retardation protein: A paradigm for translational control by RNA-binding proteins. Biochimie, 114, 147-154.
- 120. Kim, N. S., Ringeling, F. R., Zhou, Y., Nguyen, H. N., Temme, S. J., Lin, Y. T., ... & Ming, G. L. (2022). CYFIP1 dosages exhibit divergent behavioral impact via diametric regulation of NMDA receptor complex translation in mouse models of psychiatric disorders. Biological psychiatry, 92(10), 815-826.
- 121. Lei, Z., Wang, J., Zhang, L., & Liu, C. H. (2021). Ubiquitination-dependent regulation of small GTPases in membrane trafficking: from cell biology to human diseases. Frontiers in Cell and Developmental Biology, 9, 688352.
- 122. Liu, S., & Storrie, B. (2015). How Rab proteins determine Golgi structure. International review of cell and molecular biology, 315, 1-22.

- 123. Egea, G., Lázaro-Diéguez, F., & Vilella, M. (2006). Actin dynamics at the Golgi complex in mammalian cells. Current opinion in cell biology, 18(2), 168-178.
- 124. Makhoul, C., Gosavi, P., & Gleeson, P. A. (2019). Golgi dynamics: the morphology of the mammalian Golgi apparatus in health and disease. Frontiers in Cell and Developmental Biology, 7, 112.
- 125. Marra, P., Salvatore, L., Mironov Jr, A., Di Campli, A., Di Tullio, G., Trucco, A., ... & De Matteis, M. A. (2007). The biogenesis of the Golgi ribbon: the roles of membrane input from the ER and of GM130. Molecular biology of the cell, 18(5), 1595-1608.
- 126. Mitchell, S. B., Iwabuchi, S., Kawano, H., Yuen, T. M. T., Koh, J. Y., Ho, K. D., & Harata, N. C. (2018). Structure of the Golgi apparatus is not influenced by a GAG deletion mutation in the dystonia-associated gene Tor1a. Plos one, 13(11), e0206123.
- 127. Puthenveedu, M. A., & Linstedt, A. D. (2001). Evidence that Golgi structure depends on a p115 activity that is independent of the vesicle tether components giantin and GM130. The Journal of cell biology, 155(2), 227-238.
- 128. Kondylis, V., & Rabouille, C. (2003). A novel role for dp115 in the organization of tER sites in Drosophila. The Journal of cell biology, 162(2), 185-198.
- 129. Saenz, J. B., Sun, W. J., Chang, J. W., Li, J., Bursulaya, B., Gray, N. S., & Haslam, D. B. (2009). Golgicide A reveals essential roles for GBF1 in Golgi assembly and function. Nature chemical biology, 5(3), 157-165.
- 130. Sridharan, S., Jain, K., & Basu, A. (2011). Regulation of autophagy by kinases. Cancers, 3(2), 2630-2654.

- 131. 131- Lim, S., Smith, K. R., Lim, S. T. S., Tian, R., Lu, J., & Tan, M. (2016). Regulation of mitochondrial functions by protein phosphorylation and dephosphorylation. Cell & bioscience, 6(1), 1-15.
- 132. Powell, S. K., O'Shea, C., Townsley, K., Prytkova, I., Dobrindt, K., Elahi, R., ... & Brennand, K. J. (2021). Induction of dopaminergic neurons for neuronal subtype-specific modeling of psychiatric disease risk. Molecular Psychiatry, 1-13.
- 133. Kuang, X. Y., Jiang, H. S., Li, K., Zheng, Y. Z., Liu, Y. R., Qiao, F., ... & Shao, Z. M. (2016). The phosphorylation-specific association of STMN1 with GRP78 promotes breast cancer metastasis. Cancer Letters, 377(1), 87-96.
- 134. Ghilarducci, K., Cabana, V. C., Harake, A., Cappadocia, L., & Lussier, M. P. (2022).

  Membrane Targeting and GTPase Activity of Rab7 Are Required for Its Ubiquitination by RNF167. International journal of molecular sciences, 23(14), 7847.